In presenting the dissertation as a partial fulfillment of the requirements for an advanced degree from the Georgia Institute of Technology, I agree that the Library of the Institute shall make it available for inspection and circulation in accordance with its regulations governing materials of this type. I agree that permission to copy from, or to publish from, this dissertation may be granted by the professor under whose direction it was written, or, in his absence, by the Dean of the Graduate Division when such copying or publication is solely for scholarly purposes and does not involve potential financial gain. It is understood that any copying from, or publication of, this dissertation which involves potential financial gain will not be allowed without written permission.

_____

3/17/65
b

# TRANSIENT FILM BOILING ON A HORIZONTAL CYLINDRICAL SURFACE IN A SUBCOOLED LIQUID

A THESIS

Presented to

The Faculty of the Graduate Division

by

Howard Hong-Yuang Yen

In Partial Fulfillment

of the Requirements for the Degree

Doctor of Philosophy in the School of Mechanical Engineering

Georgia Institute of Technology

July, 1968

TRANSIENT FILM BOILING ON A HORIZONTAL

CYLINDRICAL SURFACE IN A SUBCOOLED LIQUID

Approved:

Chairman

Date approved by Chairman: 11 July 1968

# ACKNOWLEDGMENTS

The author wishes to express his sincere appreciation to all those who assisted in making this investigation possible.

Sincere gratitude is expressed to Dr. T. W. Jackson for his enthusiasm, friendship, and tireless efforts, which served as a source of encouragement throughout this research, and which could not have been undertaken without his advice. The time and constructive advice given by the other thesis committee members, Dr. N. W. Snyder and Dr. G. T. Colwell, are also appreciated.

A special note of thanks is due to Dr. S. P. Kezios, who maintained an active interest during this research and made invaluable suggestions regarding it. The author also wishes to express his appreciation to his former academic advisor, Dr. J. E. Sunderland, for his constant encouragement throughout his graduate study.

For his complete cooperation in sharing equipment and experiences in the experimental phase of the investigation, thanks are extended to Dr. D. R. Pitts. Indebtedness is also expressed to Mr. E. L. Richards, for his proof-reading of this thesis.

Funds provided by the National Science Foundation (Grant GK-1416) to carry out this investigation are acknowledged.

The author is indebted to his wife, Frances, for her encouragement, patience, understanding, and the sacrifices that both she and our children made during the years of graduate study.

TABLE OF CONTENTS

TABLE OF CONTENTS (Continued)

# LIST OF TABLES

# LIST OF FIGURES

LIST OF FIGURES (Continued)

# NOMENCLATURE

| Symbol | | Units |
|---|---|---|
| $A$ | phase growth constant of proportionality defined by Equation (4.47) | dimensionless |
| $C_1, C_2$ | constants used in solution of energy equation in vapor phase | dimensionless |
| $C_p$ | specific heat at constant pressure | Btu/lb.$^{\circ}$F |
| $D$ | diameter | in. |
| $d_1$ | actual wire diameter | in. |
| $d_2$ | projected wire diameter | in., cm |
| $d_3$ | projected vapor cylinder diameter | in., cm |
| $d_4$ | vapor-liquid interfacial definition error | in. |
| $E_i$ | exponential integral function defined by Equation (4.39) | dimensionless |
| $f$ | function of time defined by Equation (4.11) | in.$^2$/sec. |
| $h_{fg}$ | heat of vaporization | Btu/lb. |
| $I$ | function defined by Equation (A.4) | dimensionless |
| $k$ | thermal conductivity | Btu/sec.in.$^{\circ}$F |
| $L$ | vapor cylinder total length | in. |
| $M$ | constant used in solution of energy equation in liquid phase | dimensionless |
| $m$ | variable of measurement in error analysis | - |
| $N$ | constant used in solution of energy equation in liquid phase | dimensionless |
| $p$ | argument in $\Gamma$-function defined by Equation (A.4) static pressure | dimensionless psi |
| $\dot{q}$ | heat flux per unit length of wire | Btu/in. sec. |

| Symbol | | Units |
|---|---|---|
| $R$ | vapor-liquid interfacial radius | in. |
| $\dot{R}$ | vapor-liquid interfacial velocity | in./sec. |
| $r$ | radius | in. |
| $T$ | temperature | $^{o}F$ |
| $t$ | time<br>dummy variable of integration in gamma function | second<br>dimensionless |
| $u$ | argument in $\Gamma$-function defined by Equation (A.4) | dimensionless |
| $v$ | velocity | in./sec. |
| $x$ | dummy variable of integration, Equation (4.25) and Equation (A.3) | dimensionless |
| $y$ | dummy variable of integration, Equation (4.39) | dimensionless |

Greek Letter Symbols

| | | |
|---|---|---|
| $\alpha$ | thermal diffusivity | $in.^2/sec.$ |
| $\Gamma$ | complete gamma function defined by Equation (A.3)<br>incomplete gamma function defined by Equation (4.26) | dimensionless |
| $\eta$ | parameter defined by Equation (4.17) and Equation (4.38) | dimensionless |
| $\lambda$ | dummy variable of integration, Equation (4.22) | dimensionless |
| $\mu$ | coefficient of dynamic viscosity | lb./in. sec. |
| $\nu$ | kinematic viscosity | $in.^2/sec.$ |
| $\rho$ | density | $lb./in.^3$ |
| $\Phi$ | arbitrary mathematical function used in Equation (B.1) | - |

Subscripts

| | |
|---|---|
| $i$ | incremental unit |
| $\ell$ | refers to liquid phase |

Subscripts (continued)

| | |
|---|---|
| p | most probable |
| r | radial |
| sat | refers to saturation condition |
| v | refers to vapor phase |
| w | refers to wire |
| $\infty$ | refers to pool condition |

## SUMMARY

An analytical and experimental investigation was made to determine the transient film growth during the initial regimes of transient film boiling from a horizontal wire in subcooled liquid with various degrees of subcooling.

An analytical analysis, using the continuity, momentum, and energy equations, gives a solution for the local temperature distribution in the subcooled liquid phase; in addition, the law of the phase change front is obtained from this analysis. Incompressible, radial flow is assumed. The solution to the energy equation gives the temperature distribution as a function of the incomplete gamma function, $\tau\left(\frac{A}{2}, \frac{r^2}{4\,\alpha_\ell t}\right)$, associated with the phase growth constant of proportionality as an argument. Constant heat flux from the heat source is assumed in the vapor phase analysis. Assumption that the mode of heat transfer in the vapor phase is by conduction through the film to the vapor-liquid interface reduces the energy equation to the transient conduction equation in cylindrical coordinates, and a closed form solution for a small wire diameter is obtained. The solution to the energy equation in the vapor phase gives the temperature distribution as a function of the exponential integral function, $E_i\left(-\frac{r^2}{4\,\alpha_v t}\right)$. The energy balance at the vapor-liquid interface is obtained by applying the solutions to both the vapor and liquid phase analyses in conjunction with the energy required for vaporization at the interface. A transcendental equation obtained from energy balance gives the constant of proportionality for the law of the phase change front.

An experimental program was carried out for distilled water at various degrees of subcooling from a small diameter, horizontal, electrically heated platinum wire. An approximate step change in wire temperature was accomplished by rapid discharge of energy from an electrical capacitor into the heating element. The resulting wire temperature history closely approximated the constant heat flux requirement. The transient film growth was recorded by means of high speed motion pictures.

Wire sizes used in this study were 0.0098 inch and 0.0126 inch diameters. A total of sixteen experiments were conducted covering a range of subcooling from 5 to 43 degrees Fahrenheit.

The motion picture data were reduced to yield vapor growth rate information. This involved about 240 diameter measurements for each film for the initial ten milliseconds, after which the onset of large bubble formation at nodes along the length of the wire, typical of steady-state conditions, was evident. Volume median diameters were computed from measured data, and are presented as a function of time for the experimental runs to compare with the analytical solution.

Analytical results confirm the present experimental findings. It is also observed that the film boiling is preceded by vigorous nucleation for large heating surface temperature changes; this nucleation has a pronounced effect upon the ensuing rate of vapor formation if the bulk fluid temperature is near the saturation condition,but the effect decreases as the degree of subcooling increases.

# CHAPTER I

# INTRODUCTION

There is a current interest at the Georgia Institute of Technology in the possibility of metering small volume, periodic fluid flows by means of boiling heat transfer. This interest is concerned with fuel injection systems for internal combustion engines. The present investigation was a direct result of this interest. Also, there is a more widespread interest in transient boiling behavior because thermal systems of nuclear power reactors and high temperature quenching technique depend to a large extent on this phenomenon.

## Historical Background

The simplest form of boiling is encountered when a heated surface is exposed to a liquid at or near saturation conditions with no external agitation or force convective currents. This is generally referred to as "pool boiling." The primary correlation for steady-state boiling heat transfer data is usually expressed in the form of the boiling curve shown in Figure 1. The rather odd shape of this curve is a result of the fact that it is in actuality composed of four regimes, each representing a different mechanism of heat transfer. The existence of different regimes of boiling was first clearly discussed by Nukiyama[1] in 1934. This was the beginning of intensive efforts by many researchers throughout the scientific world to understand and explain the various phenomena associated with boiling heat transfer.

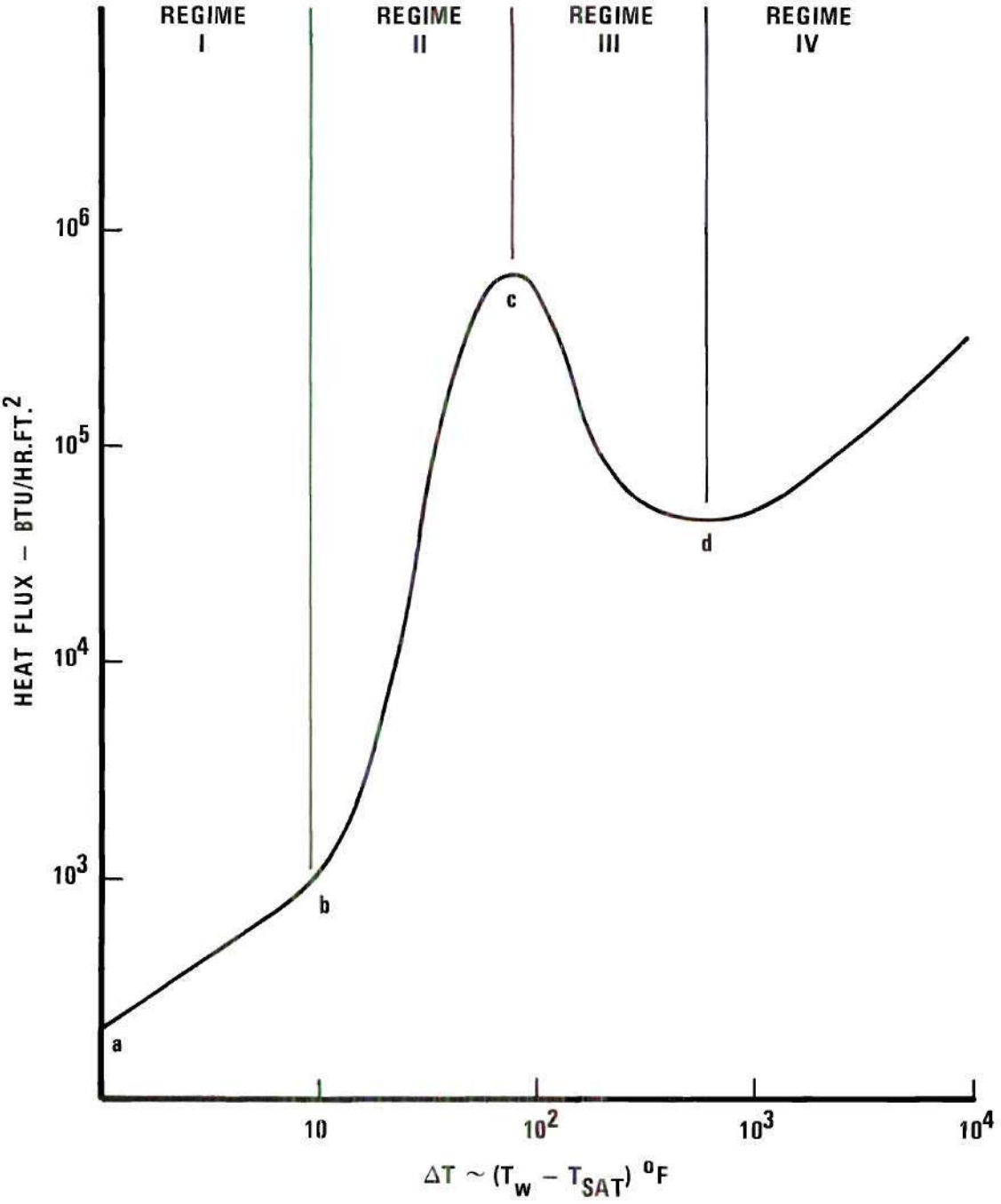


Figure 1. Typical Pool Boiling Curve for Heat Transfer from Wire to Water at Atmospheric Pressure.

In Regime I, the temperature of the surface does not exceed the boiling point of the liquid by more than a few degrees, heat is transferred to liquid near the heating surface by free convection. The convection currents circulate the superheated liquid, and evaporation takes place at the free surface of the liquid. The heat transfer mechanism in this process, although some evaporation occurs, is simply free convection, because only liquid is in contact with the heating surface. In this region the customary free convection heat transfer relationships are quite adequate to predict heat transfer.

As the temperature of the heating surface is increased such that the temperature difference between the surface and fluid saturation temperature approaches point b, phase change begins to occur in the form of bubbles at a number of favored nucleation sites on the surface. The number of such sites is dependent upon several variables; such as surface temperature and surface roughness. The mechanism of heat transfer in Regime II is very complex--heat is being removed from the surface by the vaporization process and by the high velocity convective currents associated with breakaway of the bubbles. There are many theories concerning nucleate boiling; among them, the thin film vaporization-condensation mass transfer model by Synder[2] has recently been verified by Robin[3]. We observe that, in this regime the heat flux increases rapidly with increasing surface temperature to point c. Point c has a maximum value of the heat flux, which is usually referred to as the critical heat flux or is frequently termed the "burnout point."

Increase in the excess temperature ($\Delta T = T_w - T_{sat}$) beyond point c results in transition boiling (Regime III). This is the most unusual part

of the boiling curve in that an increase in $\Delta T$ results in a decrease in the heat flux. The actual mechanism, like that of nucleate boiling is very complex. Both nucleate boiling and film boiling coexist in this regime. There is, at present, basic disagreement among researchers in this area concerning the fundamental mechanisms of transition boiling. Undoubtedly this is the least understood of the boiling regimes.

As the $\Delta T$ is increased to point d of Figure 1, the mechanism of heat transfer changes to one of stable film boiling (Regime IV). The name, "film boiling" has been given to this regime as the boiling which occurs when a complete vapor film exists between the heated surface and the liquid. Here it is generally agreed that the heat transport through the vapor film is by conduction and convection in the vapor, and by radiation through the vapor to the liquid.

For a more complete discussion of boiling heat transfer the reader is presented with the excellent reviews of Jakob[4], Kreith[5], McAdams[6], and Tong[7].

## Purpose of This Research

This research is intended to investigate the initial regime of transient film boiling from a horizontal wire in subcooled liquid with various degrees of subcooling. The primary objectives are to obtain sufficient experimental data regarding this phenomenon, and to develop an analytical expression which represents the transient film growth during this initial regime when film can be described as cylindrical.

## Related Literature

A rather limited effort has been made in the area of transient

boiling. Most of the work undertaken has been concerned with the prediction of heating surface temperatures during transients, the majority of which has been further restricted to nucleate boiling. Cole[8] conducted one of the earliest investigations of transient boiling phenomena. He was primarily concerned with the determination of temperatures developed in a ribbon type heating element. McLean, et al.[9] conducted an experimental investigation of transient boiling on a submerged horizontal wire. They utilized a very high heat flux of extremely short time duration (one microsecond), but no quantitative film growth data were obtained. Rosenthal and Miller[10] conducted an experimental investigation of heat transfer to subcooled water under transient conditions. The primary object of their investigation was to determine the heater surface temperature. The range of experiments included film boiling, but no void formation data were presented. Hamill and Bankoff[11,12] used a plane surface model and assumed heat transfer through a continuous vapor film to occur due to conduction and convection.

H. A. Johnson, et.al.[13] obtained experimental values of surface temperatures and volumes of vapor produced during transient nucleate boiling from metal ribbons. Exponentially increasing heat flux rates were employed and the transient pulses ranged from 5 to 80 milliseconds. Laurie and Johnson[14] investigated transient boiling on a vertical surface. The region of interest was the non-boiling through the nucleate boiling regimes. Graham[15] conducted an experimental study of transient nucleate boiling on a horizontal surface. He studied thermal layer thickness in a subcooled liquid.

Pitts[16] obtained experimental values of vapor growth rate for

transient film boiling and compared these with his theoretical solution, but both his experiment and theory were limited to saturated liquids.

In summary, there appears to be no quantitative experimental data for the film boiling vapor growth rate in subcooled liquids, and no theoretical analysis of transient film growth in subcooled liquids exists for the geometry of the present investigation.

# CHAPTER II

# EXPERIMENTAL EQUIPMENT

## General

An experimental analysis was conducted to complement the analytical study of transient film boiling. The fluid used was water. A brief description of the apparatus is given in this chapter. For a more detailed description and discussion of the apparatus, the reader is referred to the work of Pitts[16].

## General Requirements for Experimental Facility

The basic system required for investigation of transient film boiling has three primary requirements: (a) provision for rapid transfer of energy to the boiling heater element to minimize time duration in the nucleate regime, (b) the capability for determination of the heater element temperature history, and (c) a means for determination of the rate of vapor formation. Equipment which satisfies the above requirements is discussed in the following sections.

## Transient Film Boiling System

### Electrical Design

The primary elements of this system are:

- $R_1$ - the heater element
- 100 microfarad main energy capacitor
- 900 VDC power supply

- Ignitron power tube
- Low voltage battery
- Silicon rectifier
- Wheatstone bridge
- Oscilloscope - storage type

The primary features of this system were the simultaneous firing of current due to the discharge of the main capacitor by means of an ignitron power tube and recording of the Wheatstone bridge unbalance on the oscilloscope. The electrical schematic of this system is presented in Figure 2. The recorded Wheatstone bridge unbalance in conjunction with a knowledge of the temperature coefficient of electrical resistivity of the heater element could be used to determine the element temperature history.

Heater Element Design

The heater element material selected for this investigation was commercially available pure platinum wire. This selection was based on the favorable properties of platinum for use as a resistance thermometer and its low thermal emissivity. The heater element was mounted in a plate glass tank, shown in Figure 3. The large electrodes constitute the only part of the bridge circuit which was not duplicated during the temperature calibration. This was rendered insignificant because of the extremely low electrical resistance of these electrodes.

One-eighth inch diameter brazing rod was used as the wire holder. The method of mounting the wire in the brazing rod was by installing a short section of one-eighth inch copper tubing over the end of the brazing rod. Heat flux was then applied to the copper sleeve with a small oxy-acetylene flame. The copper, having a higher melting point than the brazing rod,

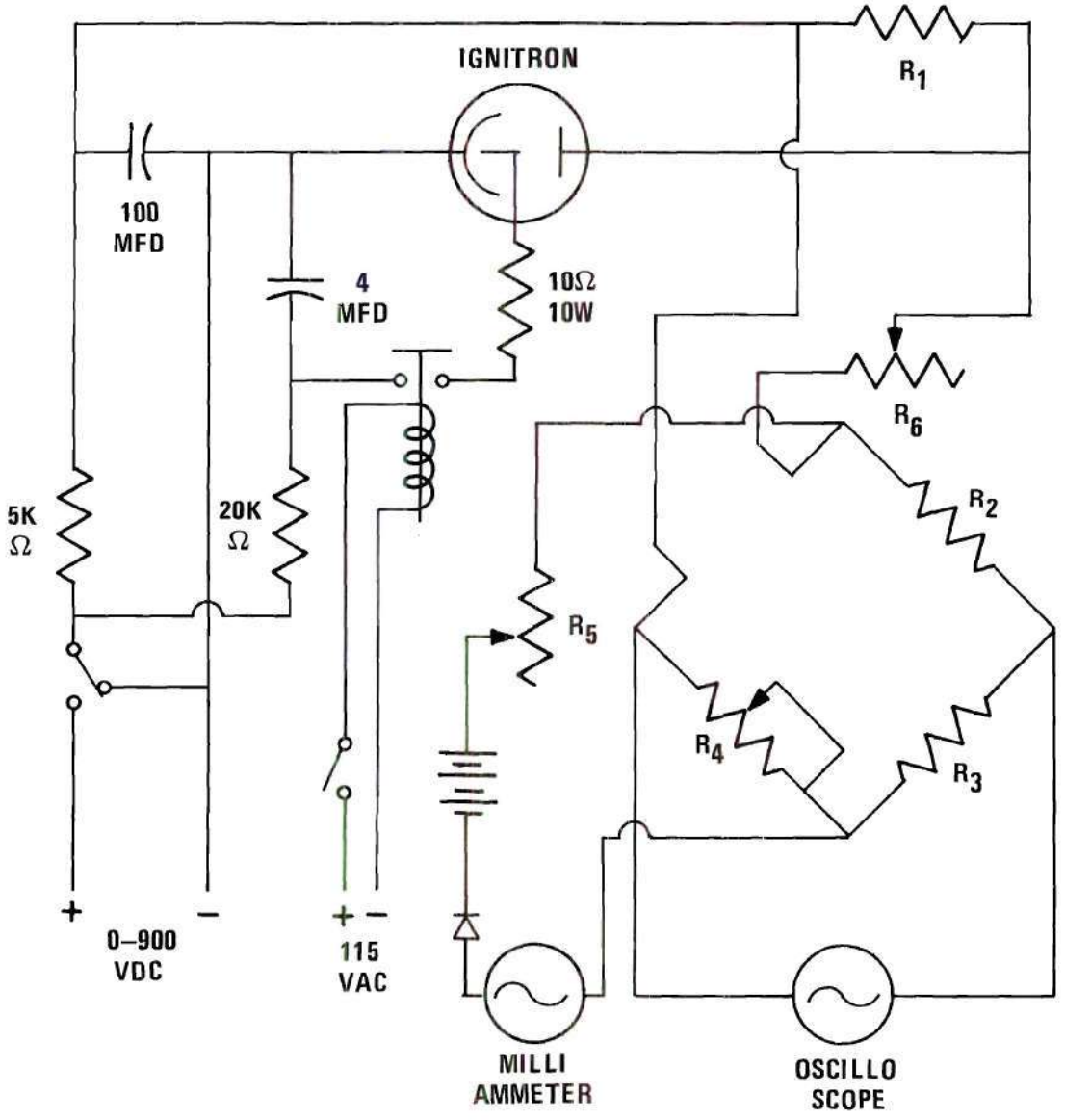


Figure 2. Transient Film Boiling System Electrical Schematic with Wheatstone Bridge Temperature Measurement System.

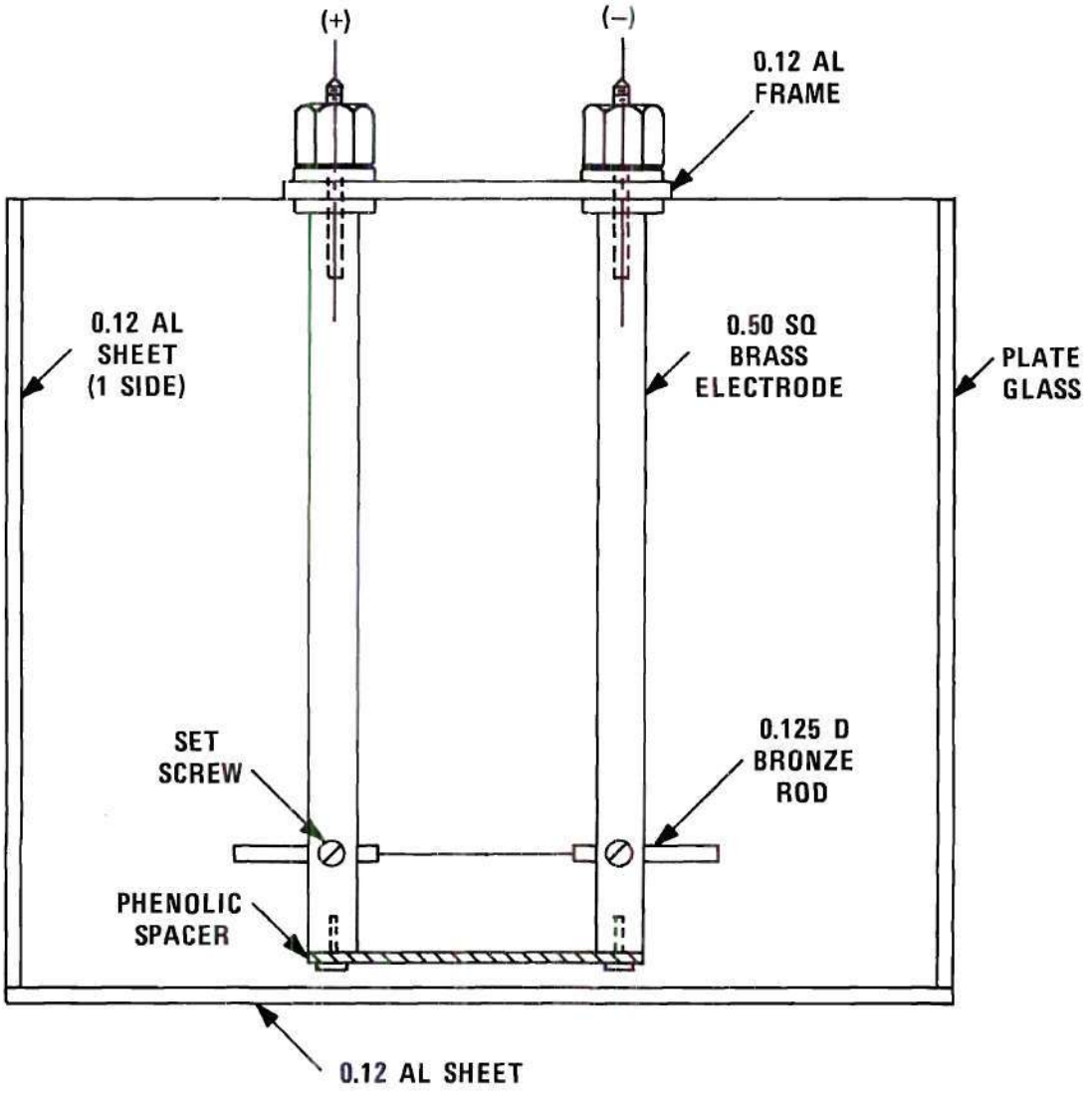


Figure 3. Test Tank Showing Electrodes and Heater Element Installation.

retained the rod material as it became liquid, and the platinum wire was inserted to a depth of approximately one-tenth inch into the molten rod. The flame was removed, and the brazed connection was allowed to cool. This configuration is shown in Figure 4.

The physical size of the heater element was governed by two factors; first, the total energy available for the element temperature step-change, and second, the loss due to end conduction of heat into the wire holders. The two-inch length was selected for the present experimental system. Detailed discussion of the wire size selection is given in the work of Pitts[16].

Test Tank Description

The boiling tank was constructed of a combination of one-eighth inch thick plate glass and aluminum. The basic tank dimensions were six inches wide by eight inches deep by ten inches long. The bottom and one end were fabricated of aluminum: this end provided a means of mounting the bulk fluid heater and thermostat. Bulk fluid heating was accomplished by means of electrical resistance heating which was sufficient to raise the fluid temperature to the saturation point. Pool temperature was maintained at desired temperature level by adjusting the voltage to the electrical resistance heater. Pool temperature was measured by three ASTM three-inch immersion thermometers in the tank. Configuration of test tank is shown in Figure 3.

Element Temperature Measurement

The element temperature method of measurement was an unbalanced Wheatstone bridge which consists of a heater wire as one of the resistances.

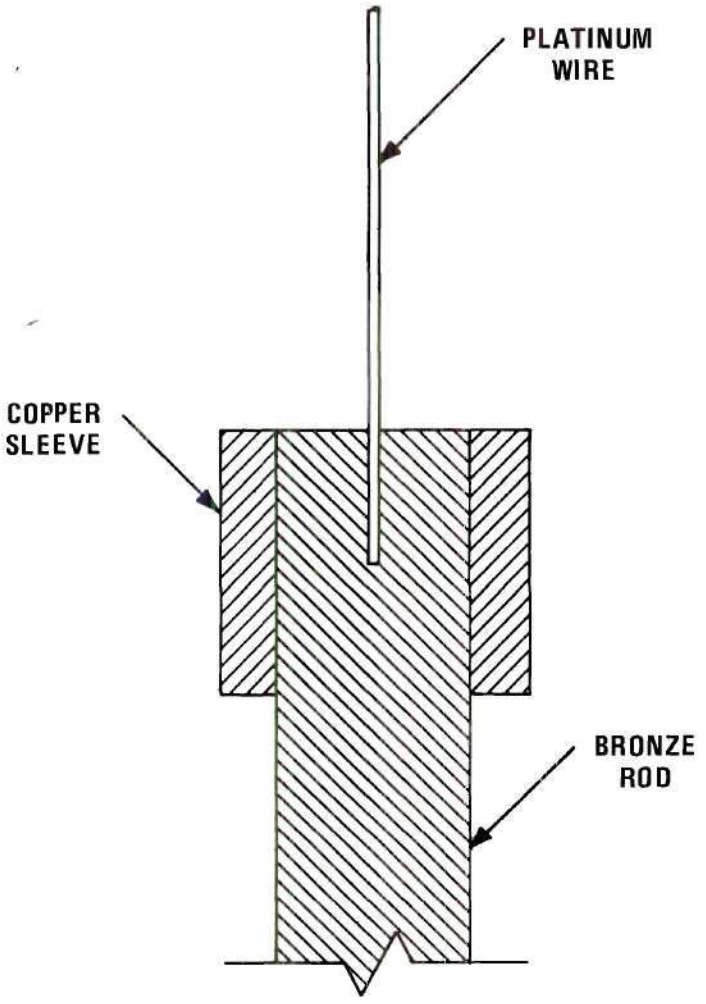


Figure 4. Heater Wire Design - Brazed to Holder.

Bridge unbalance was recorded on a Tektronix type 564 storage oscilloscope as a function of time. Prior thermometric calibration of the Wheatstone bridge unbalance as a function of temperature of the heater element was used to convert the bridge unbalance as a function of time to temperature as a function of time.

System Description

Heater Wire Selection. There are six primary material characteristics which are important for this application. These are:

1. large resistance change with temperature
2. monotonically increasing (or decreasing) resistance change with temperature
3. good brazing qualities
4. high melting temperature
5. high resistance to corrosion
6. low emissivity

Several commercial trade-named wires were considered. Pure platinum wire seems to be most satisfactory and is more readily available than most of the trade name type of wires.

Wheatstone Bridge. The bridge description is shown in Figure 5. The requirements of the design are:

1. low bridge current resulting in negligible heating of the platinum wire
2. low electrical resistance of the platinum wire compared with any other path for the capacitor energy discharge
3. high wattage resistors unaffected by the bridge current
4. milliammeter to assure application of constant bridge current

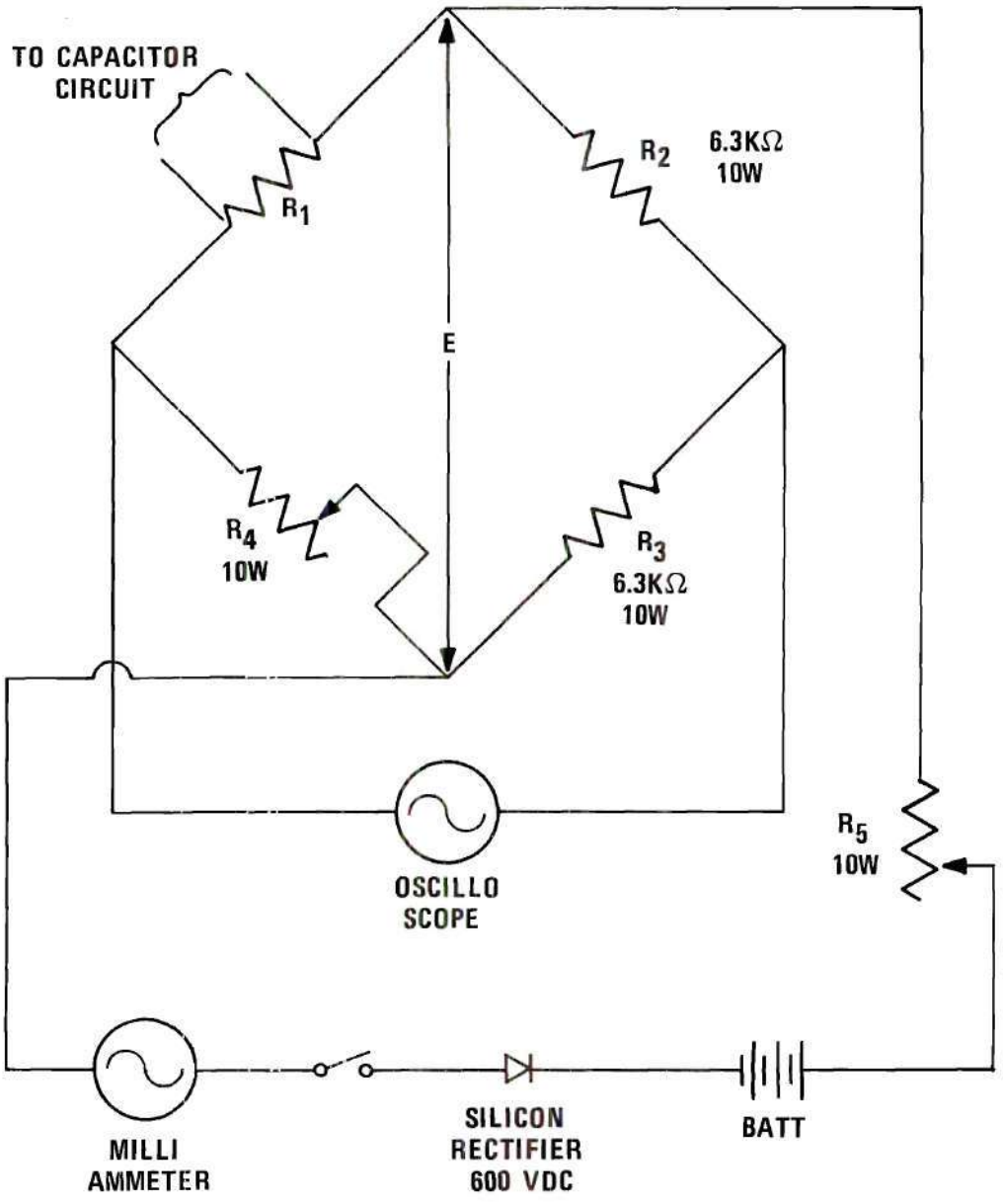


Figure 5. Schematic Diagram of Wheatstone Bridge.

regardless of battery condition.

The detailed description and discussion of this Wheatstone bridge is also given in the thesis by Pitts[16].

## Temperature Calibration Equipment

The equipment used for calibrating the Wheatstone bridge and heater element wire combination consisted of the following:

1. Thermocouple calibrating furnace, Leeds and Northrup Company, Philadelphia, Pennsylvania, Catalog No. 9003, Serial No. 1609778.
2. Certified platinum versus platinum plus 10 per cent rhodium thermocouple, Leeds and Northrup Company, Philadelphia, Pennsylvania.
3. Type K-3 potenticmeter, Leeds and Northrup Company, Philadelphia, Pennsylvania, Catalog No. 7553-6, Serial No. 1624632.
4. Electronic null detector, Leeds and Northrup Company, Philadelphia, Pennsylvania, Catalog No. 9834.
5. Unsaturated standard cell, Eppley Laboratory, Inc., Newport, Rhode Island, Catalog No. 103, Serial No. B-1608.
6. Storage oscilloscope, Tektronix, Inc., Portland, Oregon, Type 564, Serial No. 003688.
7. Differential amplifier, Tektronix, Inc., Portland, Oregon, Type 2A63, Serial No. 006627.

The platinum wire element was mounted in the center of the vertical calibration furnace by means of two No. 10 copper lead wires extending approximately 18 inches into the furnace.

The K-3 potentiometer and null detector combination was standardized

by using the standard cell. The values of electromotive force corresponding to wire temperatures were then taken from the readings of the K-3 potentiometer.

The Wheatstone bridge unbalance was read directly on the storage type oscilloscope, which was also used during the boiling experiment.

The values of electromotive force and corresponding temperatures of the platinum thermocouple junction were furnished by the Leeds and Northrup Company with this thermocouple, and they apply when the reference junctions are maintained at 32 degrees Fahrenheit.

## Photographic Equipment

High speed motion picture and associated lighting and timing equipment were used in this investigation. Equipment consisted of the following:

1. HYCAM model K1004E 16 millimeter camera and accessories marketed by Red Lake Labs, Inc., Santa Clara, California.
2. Red Lake model TLG-3 Millimite timing light generator.
3. f/1.4 Cosmicar Television Lens, Serial No. 14757.
4. Red Lake Laboratories model RLLi-1 lighting unit.
5. Two or three photo-DXB 500 watt photo-spot bulbs.

The detailed description and operational procedure for the equipment are given by Pitts[16].

Data reduction from the processed film was accomplished with a Bell and Howell model 173 time and motion study projector, Serial No. AJ92065. This unit was equipped with a Bell and Howell f/1.9 1-inch, Increlite projection lens. The two features of this projector which were of most convenience are the provision for projection of individual frames and the

frame counter which is directly coupled to the film sprocket

Heater element wire diameters were measured with a micrometer having 0.001-inch scale division, and with a Bausch and Lomb Company model DR-25, direct measuring, pre-calibrated instrument. This unit reads to 0.0001-inch.

# CHAPTER III

# EXPERIMENTAL PROCEDURE

## General

A brief discussion of experimental procedure is given in this chapter. For a more complete discussion and description of experimental procedure the reader is referred to the work of Pitts[16].

## Temperature Calibration

The method of heater element temperature measurement was given in the preceding chapter.

A total of eleven heater elements were calibrated during this investigation. Only seven of these calibrations, however, were actually used in recorded transient boiling experiments. This was a consequence of the elements failing due to burn-out during preliminary runs. Calibration data for these seven elements and element descriptive information are given in Tables 2 and 3 of Appendix C. The actual temperature at any calibration point can be obtained from the thermocouple electromotive force in conjunction with the data of Table 1 which was furnished by Leeds and Northrup Company. A typical element calibration curve is presented in Figure 6.

## Film Boiling Experiments

A general schematic of the experimental arrangement is presented in Figure 7. The procedure for all experiments was essentially the same,

Table 1. Electromotive Force and Corresponding Temperature for Platinum Versus Platinum Plus 10 Per Cent Rhodium Thermocouple

| Absolute Millivolts | International 1948 | |
|---|---|---|
| | Degrees Centigrade | Degrees Fahrenheit |
| 0.000 | 0.0 | 32.0 |
| 0.143 | 25.0 | 77.0 |
| 0.299 | 50.0 | 122.0 |
| 1.000 | 146.5 | 295.7 |
| 2.000 | 264.5 | 508.1 |
| 3.000 | 373.0 | 703.4 |
| 4.000 | 476.8 | 890.2 |
| 5.000 | 577.2 | 1071.0 |
| 6.000 | 674.2 | 1245.6 |
| 7.000 | 768.4 | 1415.1 |
| 8.000 | 859.9 | 1579.8 |
| 9.000 | 948.9 | 1740.0 |
| 10.000 | 1035.8 | 1896.4 |

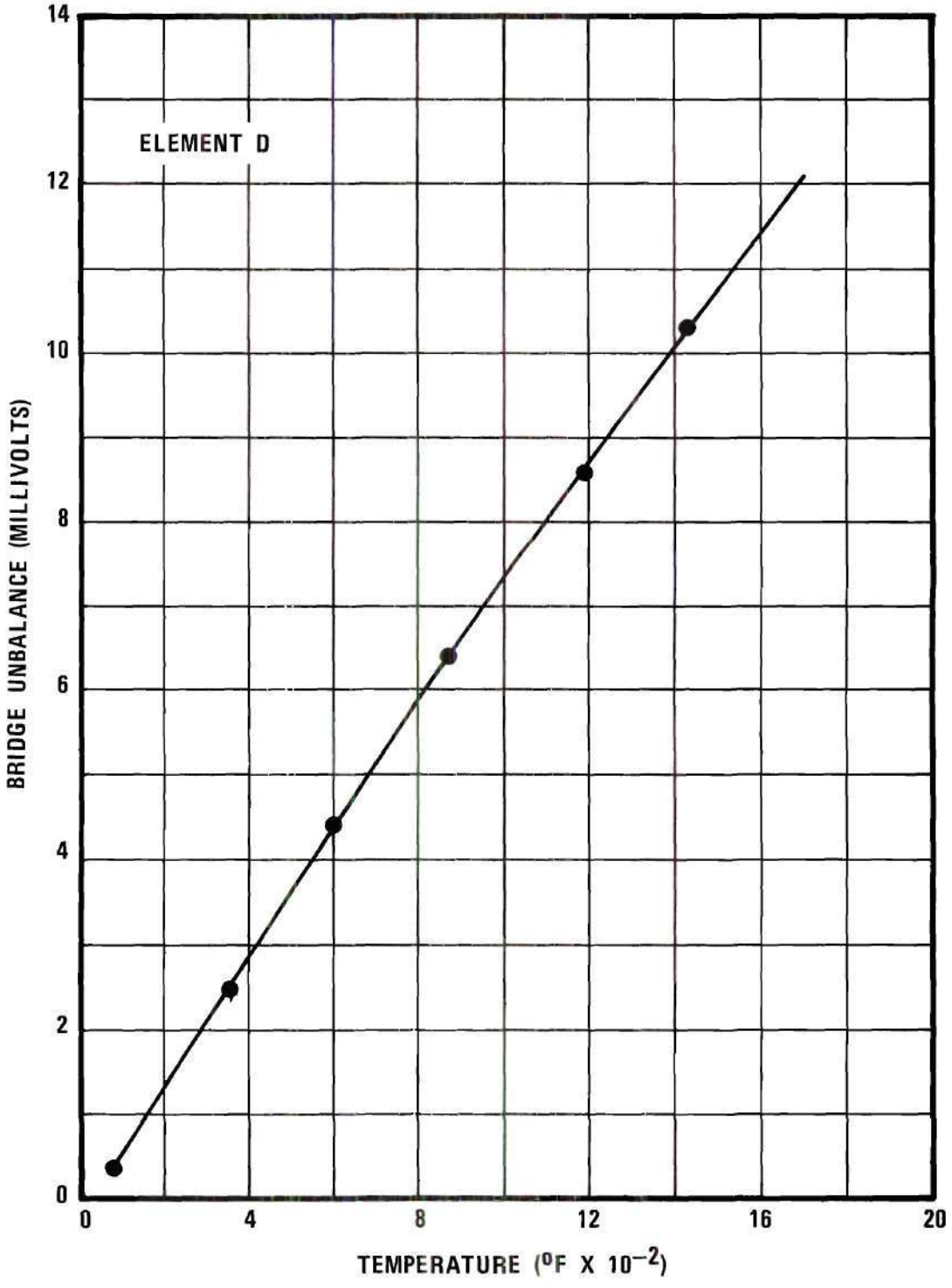


Figure 6. Typical Calibration Curve for Heater Element.

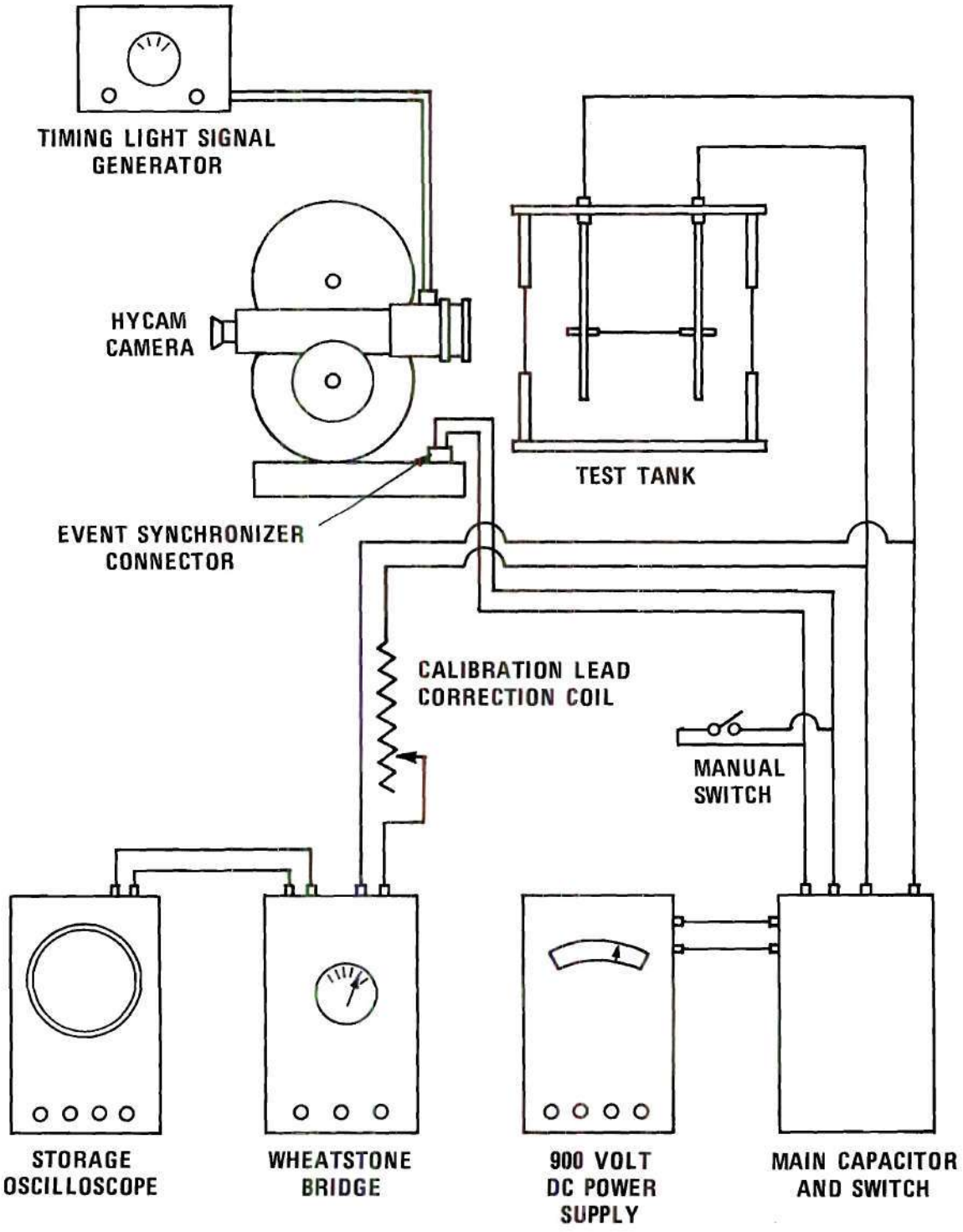


Figure 7. Schematic of General Experiment Arrangement.

and can be briefly described as follows. The boiling test tank was filled with distilled water and the fluid bulk heaters were turned on. The water was boiled vigorously for a period of not less than one hour to remove entrained gas. During this period, the camera was focused on the wire element and loaded with film. The camera framing rate was selected, and the lighting was adjusted. The oscilloscope was allowed to warm up during this pre-run boiling period. After a minimum of 30 minutes of operation, the oscilloscope was calibrated in accordance with the manufacturer's operational manual.

After the pre-run boiling period, the power supply to the fluid bulk heater was reduced to maintain pool temperature at the desired level. A zero bridge current reference line was then recorded on the oscilloscope, and the heater element Wheatstone bridge current was adjusted to the value used during element calibration. The direct current power supply was turned on and adjusted to the desired voltage. This was used to charge the main capacitor.

The capacitor was discharged by the camera synchronizer. This resulted in capacitor discharge through the heater element and automatic triggering of the oscilloscope to record the bridge unbalance as a function of time. The data recorded for each test included the following:

1. barometric pressure
2. bulk water temperature at time of capacitor discharge
3. depth of water above heater element
4. type of film
5. lens data
6. camera nominal speed setting

7. lighting data
8. Wheatstone bridge unbalance versus time
9. capacitor charge voltage
10. heater element identification

These data, for each of the reported runs, are presented in Tables 4 and 5 in Appendix C.

A total of sixteen filmed tests were conducted. Since this investigation was a continuation of Pitts[16], therefore, run numbers were given to be Runs 18 through 33. Of these, the results of nine and Run 8 of Pitts[16] were reported. With regard to the other seven, the following comments are offered.

Run 22. This test failed to produce data due to the poor lighting.

Runs 24, 25, 26, and 31. These tests were conducted with bulk fluid temperatures subcooled between 33 to 43 degrees Fahrenheit, there were no measurable vapor films formed due to the high subcooling.

Runs 28 and 31. These tests failed due to the failure of recording heater element temperature histories.

## Data Reduction

Quantitative data were obtained from high speed movie films of the transient film boiling experiments. The Bell and Howell model 173 time and motion study projector was used to measure the image of heater element wire size and vapor diameter. The ratio of the projected vapor diameter to the projected heater element size in conjunction with the measured actual wire size gave the actual vapor diameter.

The transient film growth was not truly cylindrical as discussed

by Pitts[16]. Consequently, numerous measurements were required to determine the vapor volume at any given time. The technique used involved the assumption that the vapor film could be represented as a body of revolution. Thus, the volume could be approximated by measuring the diameter at prescribed intervals along the length of the wire, calculating the area at each of these stations, multiplying this area by the distance between stations to form a volume, and summing the total of the incremental volumes thus formed. In mathematical form this is expressed as

$$v = \sum_{i=1}^{n} \frac{\pi}{4} D_i^2 \Delta \ell_i \tag{3.1}$$

$$\Delta \ell_1 = \Delta \ell_2 = \ldots \tag{3.2}$$

The accuracy of the volume thus determined is dependent upon the non-uniformity of the surface along the length and size of the incremental length chosen. The error can be reduced simply by increasing the number of measurements. For the present investigation, the total filmed length of wire was approximately three-eights of an inch. It was found that division into twenty-four length intervals resulted in a vapor volume which differed insignificantly with that obtained using thirty intervals. As a consequence, it was decided that finer division was unnecessary, and twenty-four intervals were used for data reduction for all runs.

It was decided that vapor volume at one millisecond intervals would be sufficient to represent the growth rate. Data during the first millisecond following the capacitor discharge were highly questionable due

to the nucleate character of the initial vapor formation, and consequently were neglected in the process of data reduction. The zero time point was established as being the last frame on a roll with no vapor formed. Since the framing rate for all runs was about 4000 pictures per second, the maximum time error was of the order of one-fourth millisecond. With the zero time point thus established, the time for a particular frame was determined by means of timing light blips at one millisecond intervals along the edge of the film. Using this, frames were selected for vapor volume measurement at intervals close to one millisecond.

The Bell and Howell model 173 projector was manually operated to the desired frame indicated on the continuous frame counter. Then 24-diameter measurements were taken with a scale. This procedure was repeated for frames at the selected spacing until the configuration of the vapor film indicated serious deviation toward stable film boiling. This change normally occurred at about ten milliseconds. The data thus obtained are presented in Tables 6 through 15 in Appendix C.

Using these measurements, the void volume for each frame was calculated with Equation (3.1). This volume was divided by the total length, i.e.,

$$L = \sum_{i=1}^{n} \Delta \ell_i \quad , \tag{3.3}$$

to yield the volume average area of the vapor cylinder. The volume median diameter was then determined from the volume average area.

# CHAPTER IV

# ANALYSIS

## General

It is postulated that a horizontal, cylindrical wire submerged in a liquid and at the temperature of the liquid experiences a sudden, large increase in temperature which can be represented as a step change. This temperature increase is sufficiently large to result in film boiling. Thus, the physical model for analysis is that of a uniform vapor film, initially of zero thickness, which increases with time. Eventually, the vapor liquid interface becomes quite distorted, and the model is no longer valid, but the primary concern is with the growth rate during the first ten milliseconds. For this short period, the film can be reasonably described as cylindrical. Thus, the problem can be treated as one-dimensional.

The physical model assumed is presented in Figure 8. The major assumptions in this model are:

1. The liquid is separated from the metal by a continuous vapor blanket whose thickness is independent of length.

2. The vapor-liquid interface is smooth and continuous.

3. The liquid is at saturation temperature at the liquid-vapor interface.

4. Radiative transfer of energy is negligible.

Based on the above assumptions, conservation of energy at the vapor-liquid interface can be expressed mathematically as:

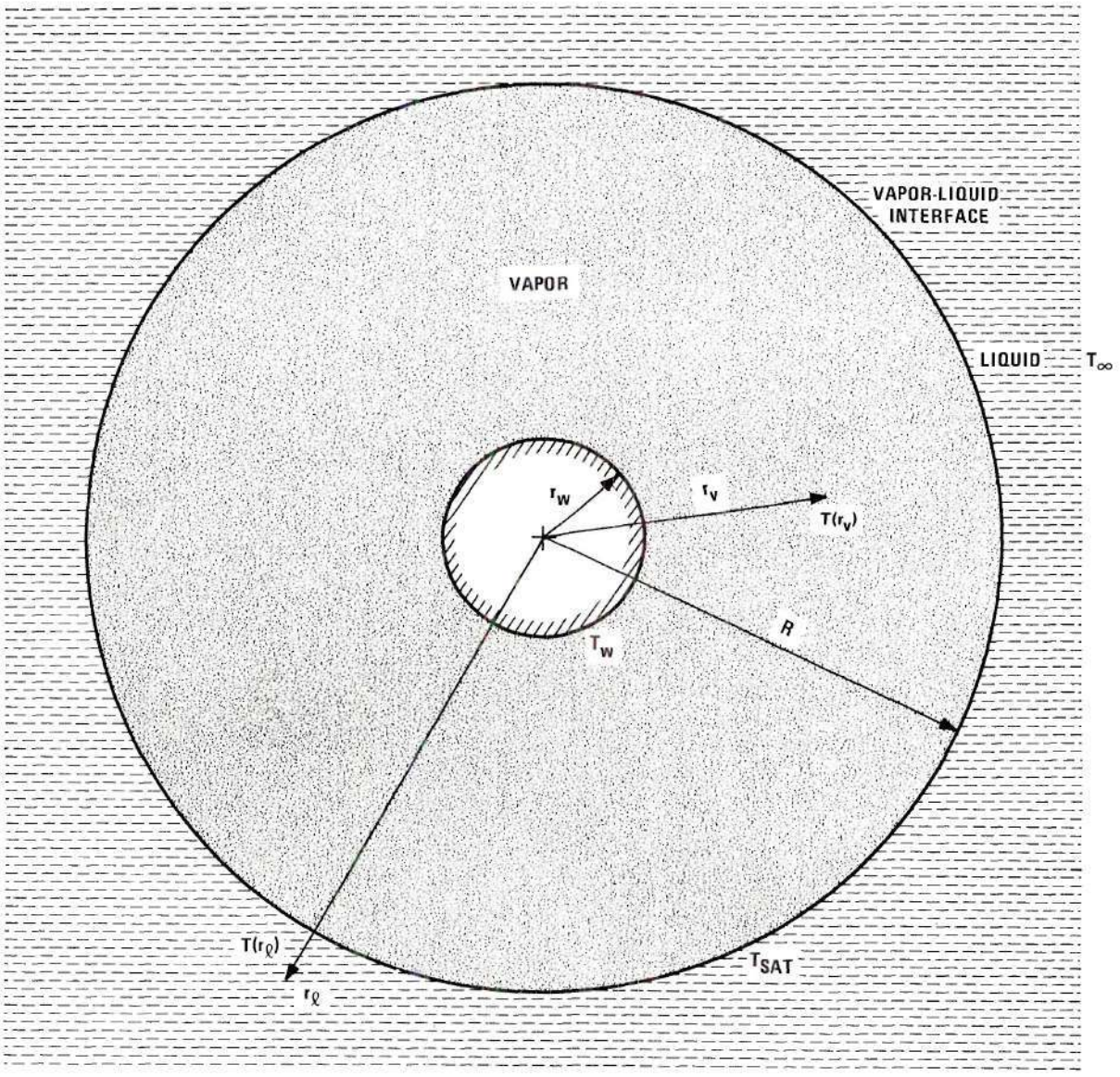


Figure 8. Physical Model for Transient film Boiling from a Cylindrical Surface.

$$\rho_v h_{fg} \dot{R} = - K_v \frac{\partial T_v}{\partial r} \Big|_R + K_\ell \frac{\partial T_\ell}{\partial r} \Big|_R \quad . \tag{4.1}$$

This expression relates the energy required to vaporize the liquid to the algebraic sum of the energy conducted to the interface through the vapor and the energy conducted away from the interface through the liquid. Equation (4.1) is derived in the thesis of Pitts[16].

Film growth rate may be obtained by solving Equation (4.1), if temperature distributions are known in both vapor and liquid phases.

## Liquid Phase Analysis

The governing equations for the liquid phase in cylindrical coordinates are:

Continuity
$$\frac{1}{r} \frac{\partial}{\partial r} (rv) = 0 \quad . \tag{4.2}$$

Momentum
$$\frac{\partial v}{\partial t} + v \frac{\partial v}{\partial r} = \nu \left[ \frac{\partial^2 v}{\partial r^2} + \frac{1}{r} \frac{\partial v}{\partial r} - \frac{v}{r^2} \right] - \frac{1}{\rho_\ell} \frac{\partial p}{\partial r} \quad . \tag{4.3}$$

Energy
$$\frac{\partial T}{\partial t} + v \frac{\partial T}{\partial r} = \alpha_\ell \left[ \frac{\partial^2 T}{\partial r^2} + \frac{1}{r} \frac{\partial T}{\partial r} \right] \quad . \tag{4.4}$$

Where:
$$\nu = \frac{\mu_\ell}{\rho_\ell} \quad \text{and} \quad \alpha_\ell = \frac{K_\ell}{\rho_\ell C_{p,\ell}} \quad ,$$

where the following assumptions have been made:

a) axial symmetry

b) no velocity or thermal variation with length

c) negligible viscous dissipation

d) negligible work of compression

e) no heat generation in the liquid

f) negligible radiation to the liquid

g) negligible body force

h) constant density

i) liquid is a Newtonian fluid

j) constant viscosity

k) constant thermal conductivity

These equations are readily obtainable from any text on fluid mechanics and heat transfer by application of the listed assumptions.

The boundary conditions on the momentum equation are:

$$r = \infty : p(\infty,t) = p_{\infty}, \quad v(\infty,t) = v_{\infty} \tag{4.5}$$

$$r = R : v(R,t) = \dot{R} \quad , \tag{4.6}$$

where the second condition can be shown to apply if the density of the vapor is negligible in comparison with the density of the liquid. The boundary conditions on the energy equation are:

$$r = \infty : T(\infty,t) = T_{\infty} \tag{4.7}$$

$$r = R : T(R,t) = T_{sat} \quad . \tag{4.8}$$

The interfacial temperature at the vapor-liquid boundary is the saturation value regardless of the liquid bulk temperature.

Since the coefficient of $\nu$ in Equation (4.3) is just the r-derivative of Equation (4.2), it vanishes, and the phenomenon is seen to be independent of viscosity. The momentum equation then reduces to

$$\frac{\partial v}{\partial t} + v \frac{\partial v}{\partial r} = - \frac{1}{\rho_\ell} \frac{\partial p}{\partial r} \quad . \tag{4.9}$$

Since the flow has only a radial component of velocity by the listed assumptions, therefore, it is irrotational and Equation (4.9) is readily integrated along r-direction as

$$\frac{\partial}{\partial t} \int_\infty^r v dr + \frac{1}{2} \int_\infty^r \frac{\partial v^2}{\partial r} dr = - \frac{1}{\rho_\ell} \int_\infty^r \frac{\partial p}{\partial r} dr \quad . \tag{4.10}$$

From Equation (4.2) it follows that

$$v = \frac{f(t)}{r} \quad . \tag{4.11}$$

Substituting Equation (4.11) into Equation (4.10) and applying boundary conditions, Equations (4.5) and (4.6), Equation (4.10) becomes

$$\dot{f}(t) \, \ell nr \Big|_\infty^r - \frac{1}{2} \frac{[f(t)]^2}{r^2} = \frac{1}{\rho_\ell} (p_\infty - p) \quad . \tag{4.12}$$

Since r is always greater than the wire radius and $\rho$, $p_\infty$ and p are some finite values, $\dot{f}(t)$ must vanish; hence,

$$\dot{f}(t) = 0$$

or

$$f(t) = \text{constant} \quad . \tag{4.13}$$

For convenience, the constant is assumed to be $\alpha_\ell A$ and is substituted into

Equation (4.11), then the velocity distribution in the liquid phase can be expressed as

$$v = \frac{\alpha_\ell A}{r} \quad . \tag{4.14}$$

Substitution of Equation (4.14) into Equation (4.4) leads to the energy equation

$$\frac{\partial T}{\partial t} + \frac{\alpha_\ell A}{r} \frac{\partial T}{\partial r} = \alpha_\ell \left[ \frac{\partial^2 T}{\partial r^2} + \frac{1}{r} \frac{\partial T}{\partial r} \right] \quad . \tag{4.15}$$

Equation (4.15) can be rearranged to a more convenient form as

$$\frac{\partial T}{\partial t} + \frac{\alpha_\ell}{r} (A-1) \frac{\partial T}{\partial r} - \alpha_\ell \frac{\partial^2 T}{\partial r^2} = 0 \quad . \tag{4.16}$$

Equation (4.16) may be solved with the boundary conditions, Equations (4.7) and (4.8), to give the temperature distribution in the liquid phase. Under the transformation

$$\eta \equiv \frac{r}{2\sqrt{\alpha_\ell t}} \quad , \tag{4.17}$$

where it is assumed that

$$T = T(\eta) \quad . \tag{4.18}$$

Equation (4.16) becomes

$$- \frac{\eta}{2t} \frac{\partial T}{\partial \eta} + (A-1) \frac{\alpha_\ell}{2r\sqrt{\alpha_\ell t}} \frac{\partial T}{\partial \eta} - \frac{1}{4t} \frac{\partial^2 T}{\partial \eta^2} = 0 \quad , \tag{4.19}$$

after multiplication by $-4\alpha_\ell t$ we obtain

$$\frac{\partial^2 T}{\partial \eta^2} + \left[2\eta - \frac{(A-1)}{\eta}\right]\frac{\partial T}{\partial \eta} = 0 \quad . \tag{4.20}$$

Integrating Equation (4.20) yields

$$\frac{dT}{d\eta} = Me^{-\eta^2}\,\eta^{A-1} \quad . \tag{4.21}$$

A second integration gives

$$T = N + M\int e^{-\lambda^2}\,\lambda^{A-1}\,d\lambda \quad . \tag{4.22}$$

Examination of the definition of $\eta$, Equation (4.17) reveals that

$$\lim_{r \to \infty} \eta = \infty \quad , \tag{4.23}$$

and for any finite value of r at time t, the limiting value is simply $\eta$. Thus, for the present problem Equation (4.22) may be expressed as

$$T = N + M\int_{\infty}^{\eta} e^{-\lambda^2}\,\lambda^{A-1}\,d\lambda \quad , \tag{4.24}$$

which after multiplication and division of the integrand may be expressed as

$$T = N - \frac{M}{2}\int_{\eta^2}^{\infty} x^{\frac{A}{2}-1}\,e^{-x}\,dx \quad , \tag{4.25}$$

or, in terms of $\Gamma\left(\frac{A}{2},\eta^2\right)$ defined by

$$\Gamma\left(\frac{A}{2}, \eta^2\right) = \int_{\eta^2}^{\infty} x^{\frac{A}{2} - 1} e^{-x} \, dx \tag{4.26}$$

the temperature distribution is given by

$$T = N - \frac{M}{2} \Gamma\left(\frac{A}{2}, \eta^2\right) \quad . \tag{4.27}$$

Returning to the (r,t) coordinate system, the temperature is given by

$$T = N - \frac{M}{2} \Gamma\left(\frac{A}{2}, \frac{r^2}{4 \alpha_\ell t}\right) \tag{4.28}$$

with boundary conditions Equations (4.7) and (4.8). Applying Equation (4.7) to Equation (4.28) yields

$$T_\infty = N \tag{4.29}$$

and

$$T = T_\infty - \frac{M}{2} \Gamma\left(\frac{A}{2}, \frac{r^2}{4 \alpha_\ell t}\right) \quad . \tag{4.30}$$

Applying the boundary condition Equation (4.8) to Equation (4.30) yields

$$T_{sat} - T_\infty = - \frac{M}{2} \Gamma\left(\frac{A}{2}, \frac{R^2}{4 \alpha_\ell t}\right) \tag{4.31}$$

and

$$T = T_\infty + (T_{sat} - T_\infty) \frac{\Gamma\left(\frac{A}{2}, \frac{r^2}{4 \alpha_\ell t}\right)}{\Gamma\left(\frac{A}{2}, \frac{R^2}{4 \alpha_\ell t}\right)} \quad . \tag{4.32}$$

Equation (4.32) gives the temperature distribution in the liquid phase. The derivative of Equation (4.32) may be obtained by substitution of Equation (4.31) into Equation (4.21) and changing the coordinates back to the (r,t) coordinate system. The expression of this derivative is then

$$\frac{\partial T}{\partial r} = - \frac{1}{\sqrt{\alpha_\ell t}} \frac{(T_{sat}-T_\infty)}{\Gamma\left(\frac{A}{2}, \frac{R^2}{4\alpha_\ell t}\right)} \left(\frac{r}{2\sqrt{\alpha_\ell t}}\right)^{A-1} e^{-\frac{r^2}{4\alpha_\ell t}} \quad . \qquad (4.33)$$

## Vapor Phase Analysis

Several researchers have indicated that the primary mode of heat transfer in the vapor during film boiling is by conduction. Bromley[17] in his pioneering work on stable film boiling states as an assumption for his theory, "Heat travels through vapor film by conduction and radiation;" Pitts[16] used the same assumption in his analysis with negligible radiative heat transfer.

Assuming convective terms to be negligible, then the energy equation for the vapor phase may be reduced to

$$\frac{\partial T}{\partial t} = \alpha_v \left[ \frac{\partial^2 T}{\partial r^2} + \frac{1}{r} \frac{\partial T}{\partial r} \right] \quad , \qquad (4.34)$$

where the following assumptions have been made:

a) axial symmetry

b) no velocity or thermal variation with length

c) negligible work of compression

d) negligible radiation to the vapor

e) no heat generation in the vapor

f) constant thermal conductivity

The boundary conditions on the energy equation are:

$$r \to 0 : \dot{q} = - 2 \pi r K_v \frac{\partial T}{\partial r} \Big|_{r \to 0} \tag{4.35}$$

$$r = R \; ; \; T(R,t) = T_{sat} \quad , \tag{4.36}$$

where the wire radius is assumed to be negligible and the vapor temperature at the vapor-liquid boundary is the saturation value regardless of the liquid bulk temperature.

The general solution to Equation (4.34) is readily available from Carslaw and Jaeger[18] or Pitts[16]. The solution is given as

$$T = C_1 + C_2 \, E_i \, (-\eta^2) \tag{4.37}$$

where

$$\eta = \frac{r}{2\sqrt{\alpha_v t}} \tag{4.38}$$

and

$$-E_i(-\eta^2) = \int_{\eta^2}^{\infty} \frac{e^{-y}}{y} \, dy \quad . \tag{4.39}$$

Applying the boundary condition of Equation (4.36) into Equation (4.37) yields

$$T_{sat} = C_1 + C_2 \, E_i \left( - \frac{R^2}{4 \alpha_v t} \right) . \tag{4.40}$$

Applying the boundary condition of Equation (4.35) into Equation (4.37) yields

$$\dot{q} = - 4 \pi K_v C_2 \quad . \tag{4.41}$$

From Equations (4.40) and (4.41) constants $C_1$ and $C_2$ can be determined as

$$C_1 = T_{sat} + \frac{\dot{q}}{4 \pi K_v} E_i \left( - \frac{R^2}{4 \alpha_v t} \right) \tag{4.42}$$

$$C_2 = - \frac{\dot{q}}{4 \pi K_v} \quad . \tag{4.43}$$

Substitution of Equations (4.42) and (4.43) into Equation (4.37) gives the temperature distribution in the vapor phase as

$$T = T_{sat} + \frac{\dot{q}}{4 \pi K_v} \left[ - E_i \left( \frac{-r^2}{4 \alpha_v t} \right) + E_i \left( \frac{-R^2}{4 \alpha_v t} \right) \right] \tag{4.44}$$

and the derivative may be expressed as

$$\frac{\partial T}{\partial r} = - \frac{\dot{q}}{2 \pi K_v} \frac{e^{- \frac{r^2}{4 \alpha_v t}}}{r} \quad . \tag{4.45}$$

Film Growth Rate

Substitution of Equations (4.33) and (4.45) evaluated at the vapor-liquid interface into Equation (4.1) yields

$$\rho_v h_{fg} \dot{R} = \frac{\dot{q}}{2\pi} \frac{e^{-\frac{R^2}{4\alpha_v t}}}{R} - \frac{K_\ell (T_{sat}-T_\infty)}{\Gamma\left(\frac{A}{2}, \frac{R^2}{4\alpha_\ell t}\right)} \left(\frac{R}{2\sqrt{\alpha_\ell t}}\right)^{A-1} \frac{e^{-\frac{R^2}{4\alpha_\ell t}}}{\sqrt{\alpha_\ell t}} ,$$

or after rearrangement:

$$\rho_v h_{fg} \dot{R}R = \frac{\dot{q}}{2\pi} e^{-\frac{R^2}{4\alpha_v t}} - \frac{2K_\ell (T_{sat}-T_\infty)}{\Gamma\left(\frac{A}{2}, \frac{R^2}{4\alpha_\ell t}\right)} \left(\frac{R^2}{4\alpha_\ell t}\right)^{\frac{A}{2}} e^{-\frac{R^2}{4\alpha_\ell t}} . \quad (4.46)$$

This equation describes the energy balance at the vapor-liquid interface.

In the liquid phase analysis, an expression for the motion of liquid was obtained as

$$v = \frac{\alpha_\ell A}{r} . \quad (4.14)$$

If the liquid velocity is evaluated at the liquid-vapor interface, then the liquid motion also describes the motion of interface; therefore,

$$v \Big|_{r = R} = \dot{R} = \frac{\alpha_\ell A}{R}$$

or

$$\dot{R}R = \alpha_\ell A . \quad (4.47)$$

Integrating Equation (4.47) with the initial value of R equal to zero at

time zero, the interfacial motion can be obtained as a function of time and the constant A as follows:

$$R^2 = 2\,\alpha_\ell A t \quad . \tag{4.48}$$

Determination of the constant A can be accomplished by substitution of Equations (4.47) and (4.48) into Equation (4.46) and solving for A. The final result is

$$\rho_v h_{fg} \alpha_\ell A = \frac{\dot{q}}{2\pi} e^{-\frac{\alpha_\ell}{\alpha_v}\frac{A}{2}} - \frac{2K_\ell (T_{sat}-T_\infty)}{\Gamma\left(\frac{A}{2}, \frac{A}{2}\right)} \left(\frac{A}{2}\right)^{\frac{A}{2}} e^{-\frac{A}{2}} \quad . \tag{4.49}$$

This transcendental equation in A is the major result of the present analysis.

## Approximate Solution for the Small Radius Wire

There is no exact solution to this problem as pointed out by Carslaw and Jaeger[18]; therefore, certain approximations must be introduced to obtain a solution.

If the initial value of Equation (4.47) is changed to

$$t = 0 : \quad R = r_w \tag{4.50}$$

then the motion of the liquid-vapor interface may be expressed as

$$R^2 = 2\,\alpha_\ell A t + r_w^2$$

or

$$R = \sqrt{2 \alpha_{\ell} A t + r_w^2} \quad . \tag{4.51}$$

If it is assumed that the result of Equation (4.49) can be used to evaluate the constant in Equation (4.51), then the solution may be obtained. Equation (4.51) in conjunction with Equation (4.49) has been solved for all cases of the present experimental program. The results are presented in the following chapter, where the growth rate of Equation (4.51) is compared with experimental data for all runs. In addition, an example of the solution of this equation is presented in Appendix A.

# CHAPTER V

# DISCUSSION OF RESULTS

## Temperature Measurement

The measurement of heater element temperature by means of the Wheatstone bridge and oscilloscope system was satisfactory for the purpose of correlating vapor growth data. A detailed discussion of this system is given in the work of Pitts[16]. A typical experimental temperature versus time plot is presented in Figure 9. The apparent indicated wire temperature decay is linear after the first two to three milliseconds following capacitor discharge. The low value of indicated temperature during the first two to three milliseconds is attributable to the main capacitor voltage remaining above the bridge millivolt potential level for this short time period. The element temperature change is governed by the capacitor discharge, and this is better than 99 per cent complete at the end of 100 microseconds. As a consequence, the best representation of temperature is obtained by extrapolation of the linear data points back to time zero. If this temperature adjustment is made, then the temperature history in the first ten milliseconds may be approximated by a linear decay curve.

This indicates that the heat transfer rate from the heater element to the vapor phase was nearly constant during the first ten milliseconds following the capacitor discharge. Review of the temperature versus time plot for all the runs in the present investigation indicated that the

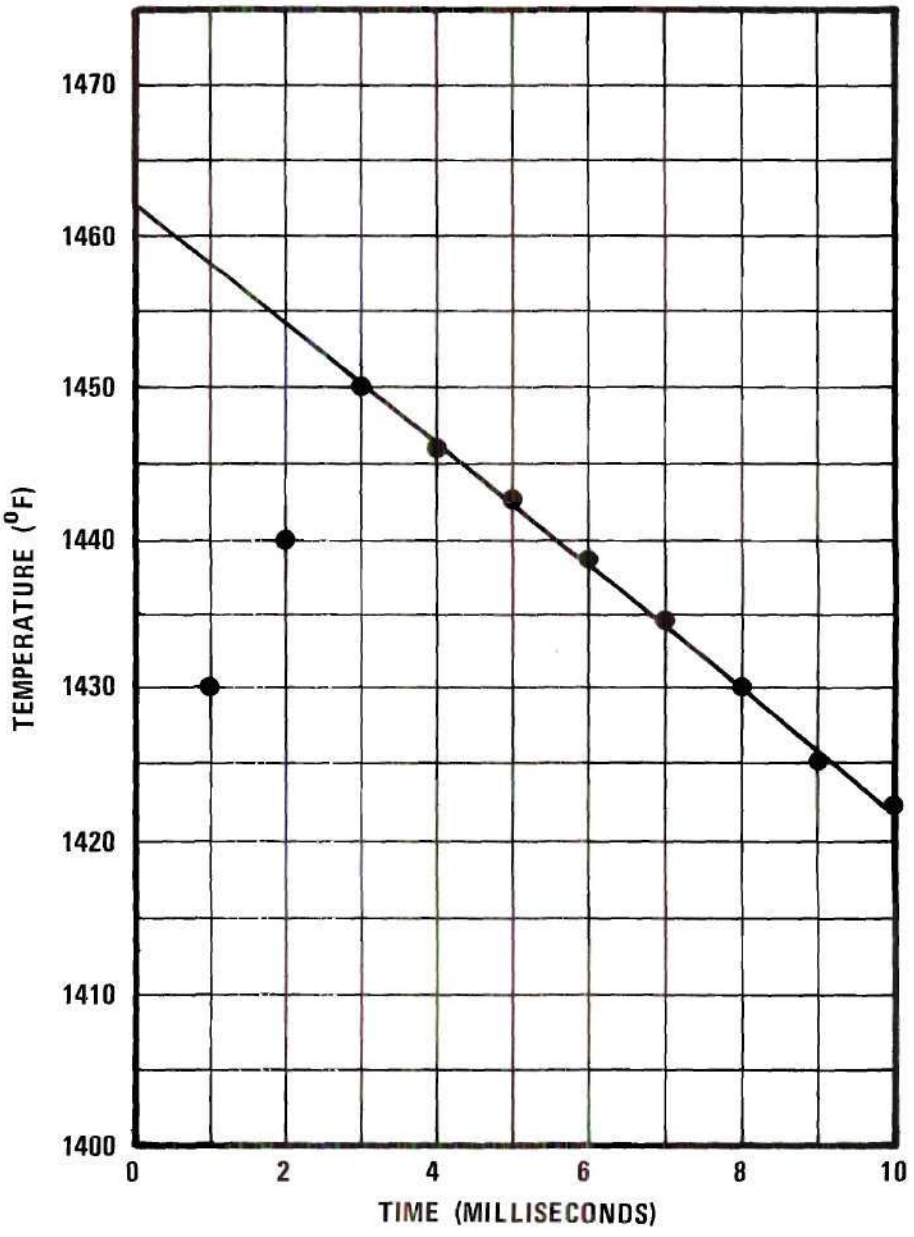


Figure 9. Heater Element Temperature Versus Time Recorded During Run 23.

constant heat flux assumption may be used in the analytical treatment. The heat flux used in the vapor growth calculation was obtained from the temperature history of each run.

## Experimental Vapor Growth Data

The filmed results for each run showed an initial burst of vapor occurring at the beginning of each experiment. This vapor is completely opaque, as opposed to the transparency of the vapor evident in the later frames for each experiment. This indicates that the initial vapor is of nucleate character. The same phenomena were observed and reported by Pitts[16].

This initial nucleation has a decided effect on the ensuing vapor cylinder growth rate if the bulk fluid temperature is nearly saturated. Experimental results of this investigation also indicated that the initial nucleation effect decreases as the degree of subcooling increases. This phenomenon may be explained by the vaporization-condensation mass transfer model of Snyder[2]. It was also observed in this investigation that if the bulk water temperature is subcooled by 40 degrees Fahrenheit, the high condensation rate of the initial nucleate bubbles prevents coalescence of bubbles to form a film. As a consequence, there is no film boiling. This has been observed even if the element temperature reaches 2000 degrees Fahrenheit.

## Analytical Solution for Vapor Growth

The results of the analysis, Chapter IV, Equations (4.49) and (4.51) have been applied to each transient film boiling experiment of the program. As previously mentioned in this chapter, heat flux is taken from the ele-

ment temperature history and is treated as a constant in the analysis.

Equation (4.49) is an expression for the energy balance at the vapor-liquid interface; therefore, in evaluating parameter A, all the properties are evaluated at the saturation condition.

The value of parameter A, which is a function of the heat flux, degree of subcooling and the thermophysical properties of vapor and liquid, has been determined for each of the runs reported herein using property values from Kreith[5] and Keenan and Keyes[19]. The vapor cylinder diameters computed from Equation (4.51) have been plotted in Figures 10 through 19 to compare with the reduced experimental data. Also, a sample solution of the transcendental equation (4.49) involving only the use of a slide rule and tabulated values of incomplete gamma function is presented in Appendix A.

Experimental runs 8, 18, 27, 29, and 30 were conducted with a wire diameter of 0.0098 inch, and runs 19, 20, 21, 23, and 32 were with a wire diameter of 0.0126 inch. Analytical results confirm the present experimental results for all runs for large times (5 milliseconds). Runs 18, 19, 20, and 29, as shown in Figures 11, 12, 13, and 17, respectively, deviated from the analytical results in the initial three to four milliseconds, these higher values of the experimental findings are due to the fact that the film boiling is preceded by vigorous nucleation if the bulk fluid temperature is near the saturation condition. Since the initial nucleation effect is less pronounced in the higher subcooled cases, the present analysis agrees with the higher subcooled cases better than the near saturation cases, as indicated by Figures 10, 14, 16, and 19.

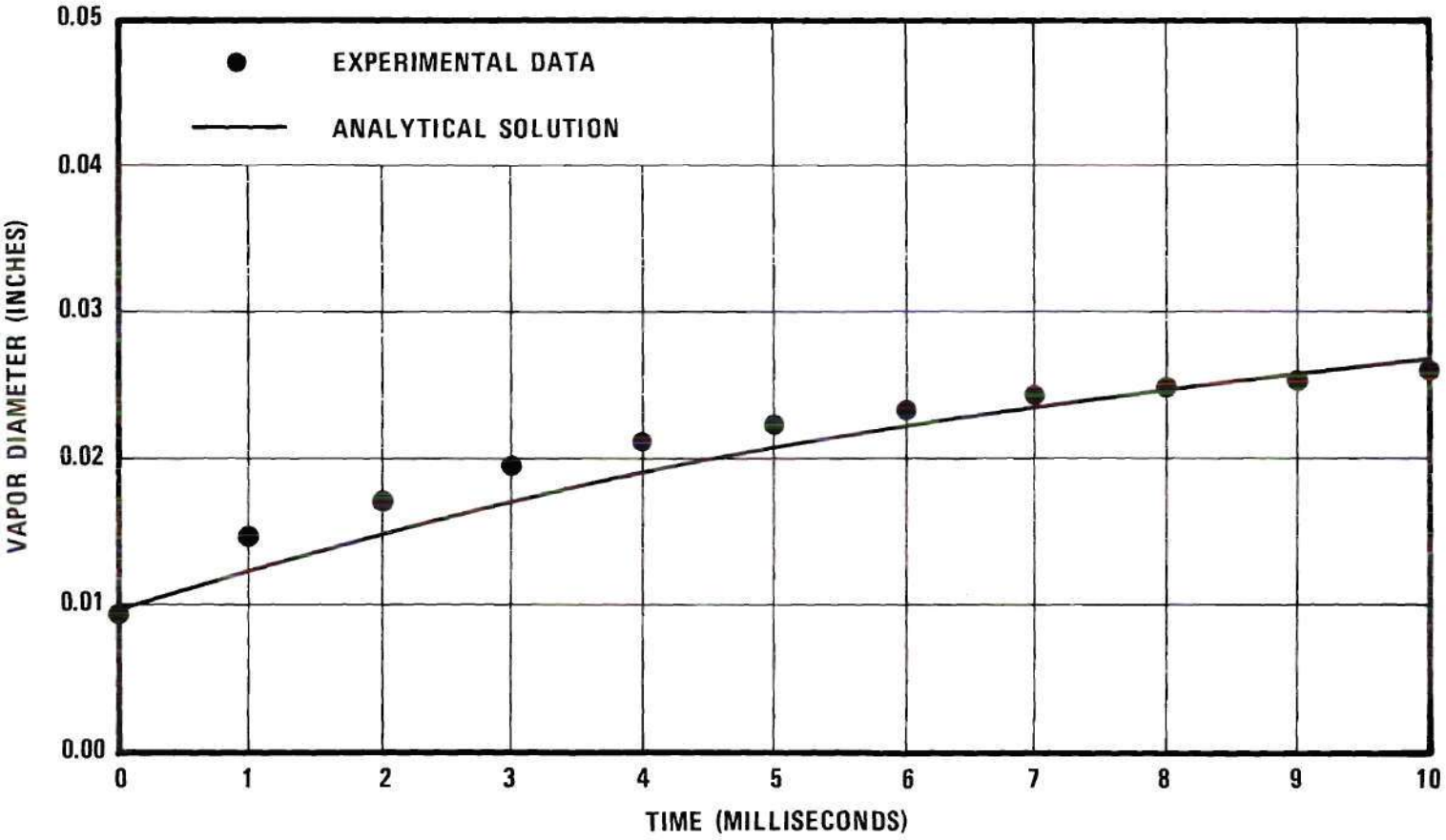


Figure 10. Plot of Vapor Diameter as a Function of Time for Run 8

$T_\infty = 194^\circ F$, $\dot{q} = 0.0167$ Btu/sec.in.

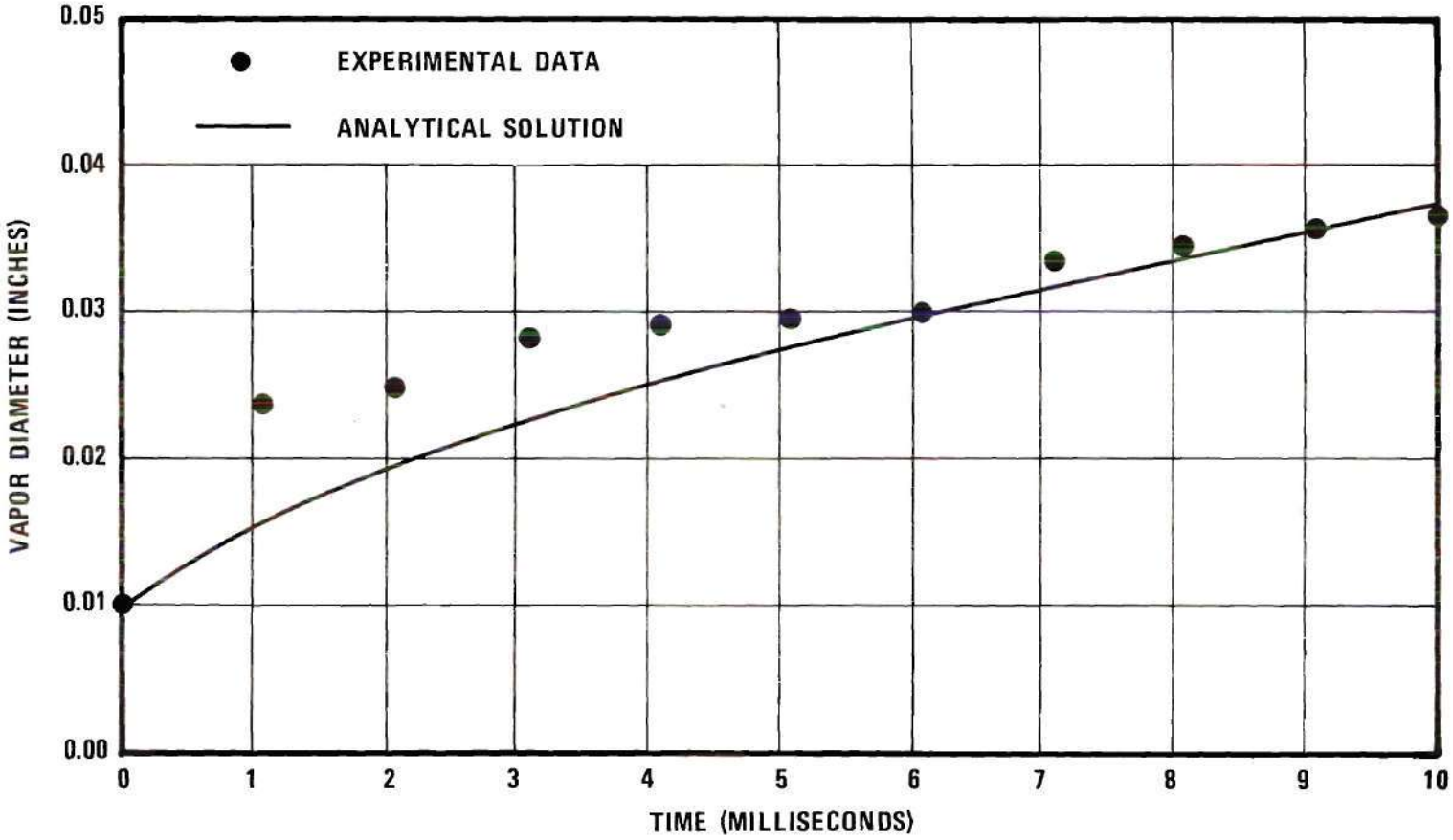


Figure 11. Plot of Vapor Diameter as a Function of Time for Run 18

$T_\infty = 203^\circ F$, $\dot{q} = 0.0246$ Btu/sec.in.

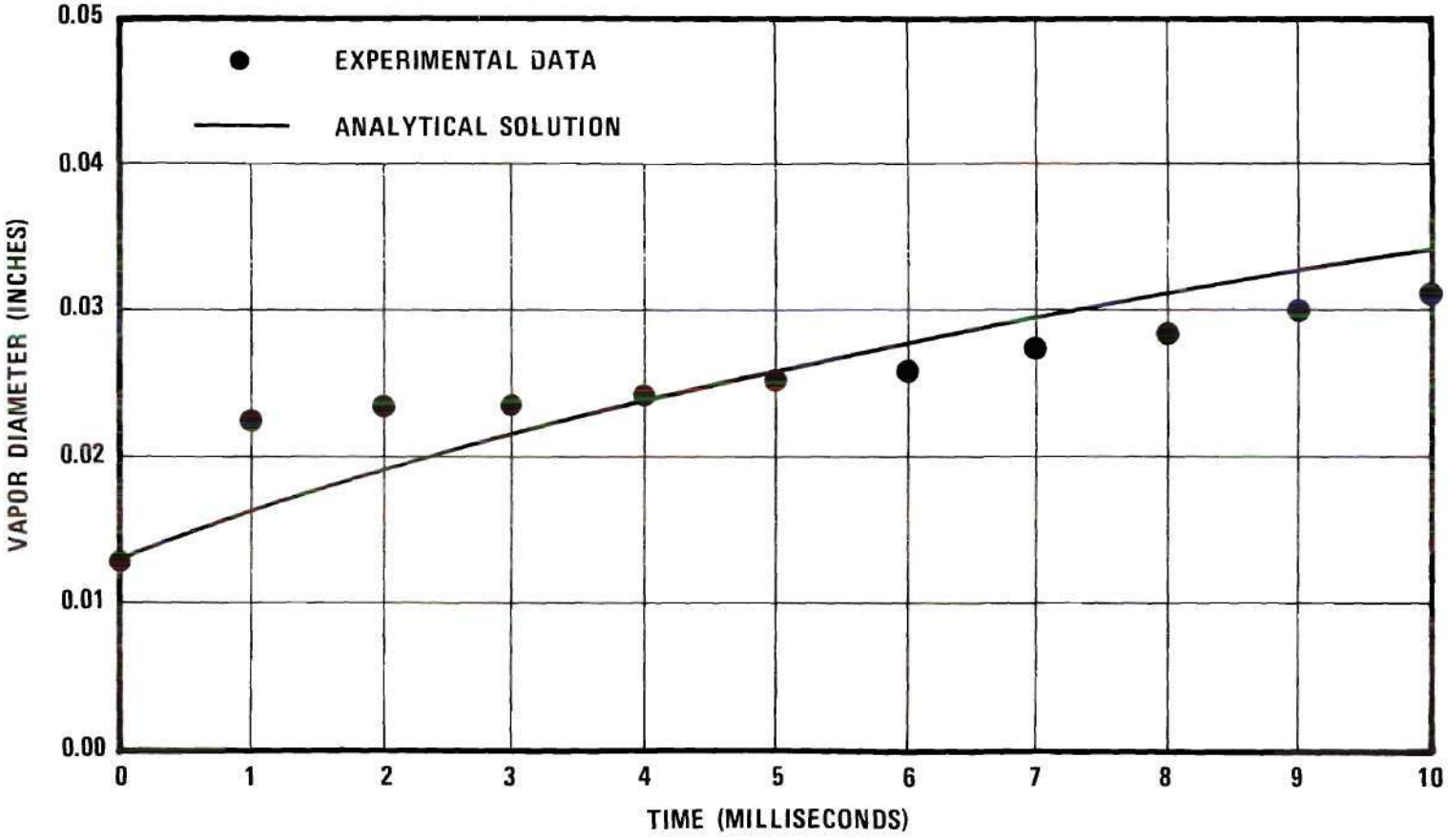


Figure 12. Plot of Vapor Diameter as a Function of Time for Run 19

$T_\infty = 202.5^\circ F$, $\dot{q} = 0.0142$ Btu/sec.in.

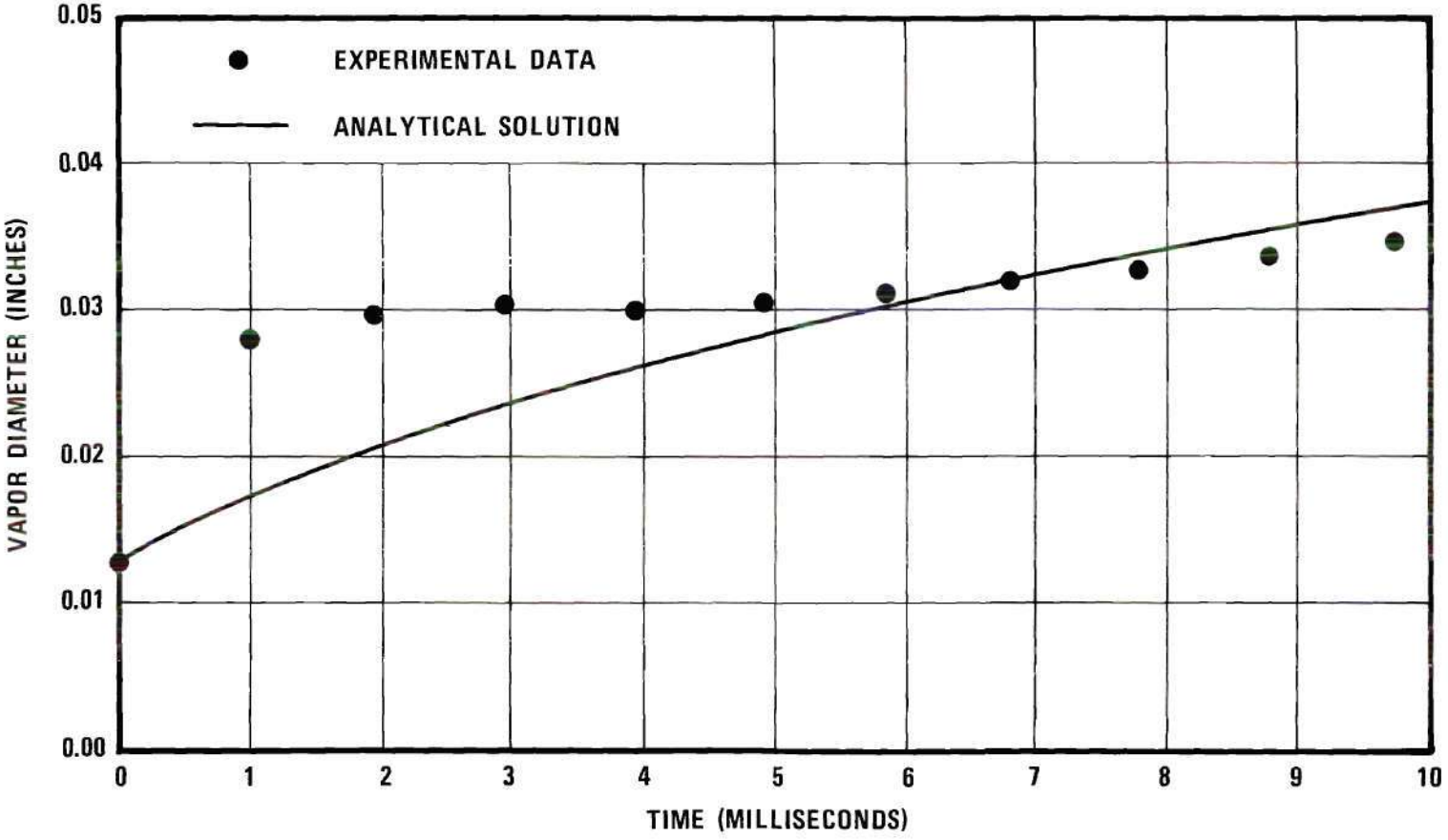


Figure 13. Plot of Vapor Diameter as a Function of Time for Run 20

$T_\infty = 205^\circ F$, $\dot{q} = 0.0203$ Btu/sec.in.

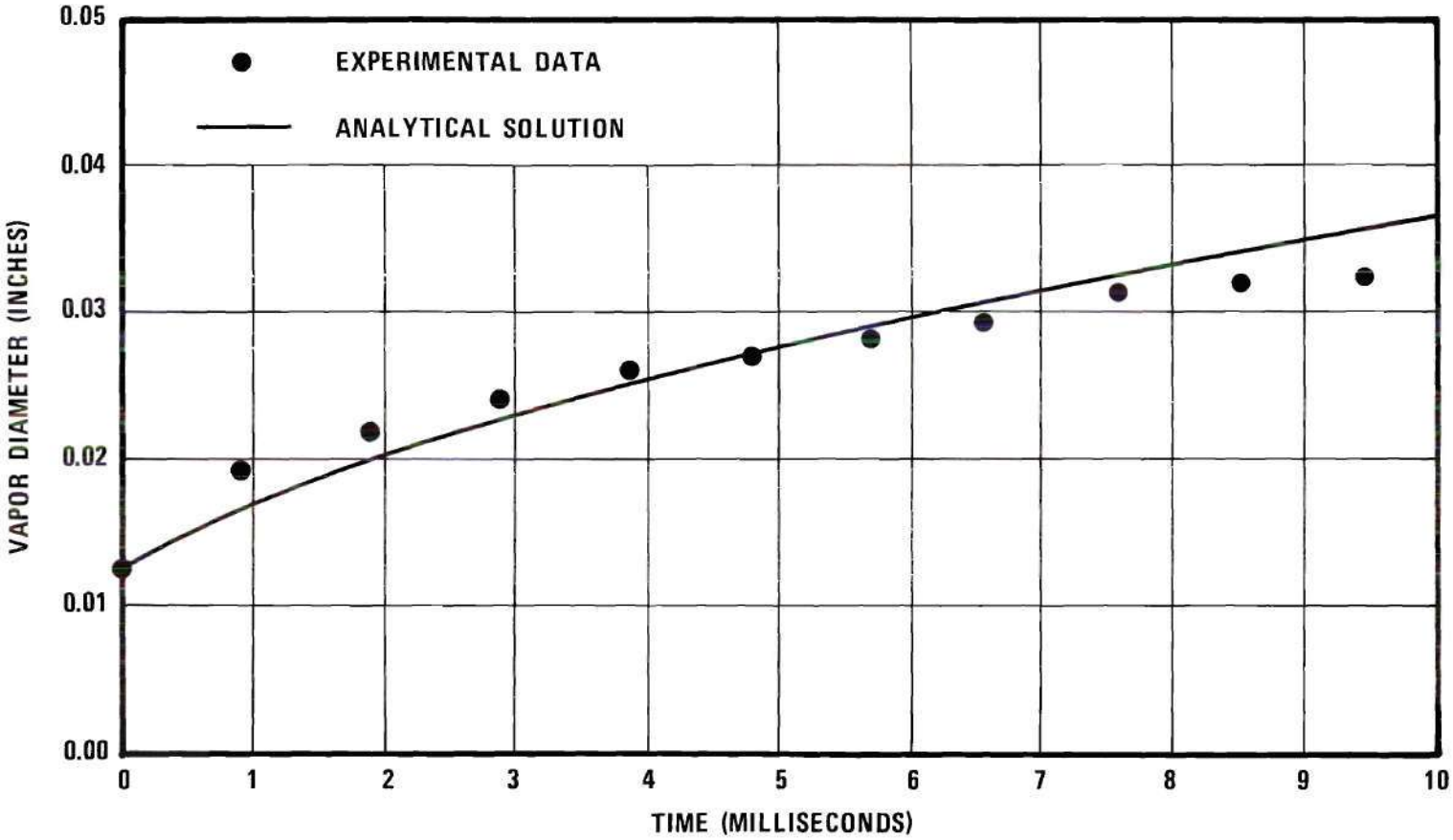


Figure 14. Plot of Vapor Diameter as a Function of Time for Run 21

$T_\infty = 192^\circ F$, $\dot{q} = 0.0464$ Btu/sec.in.

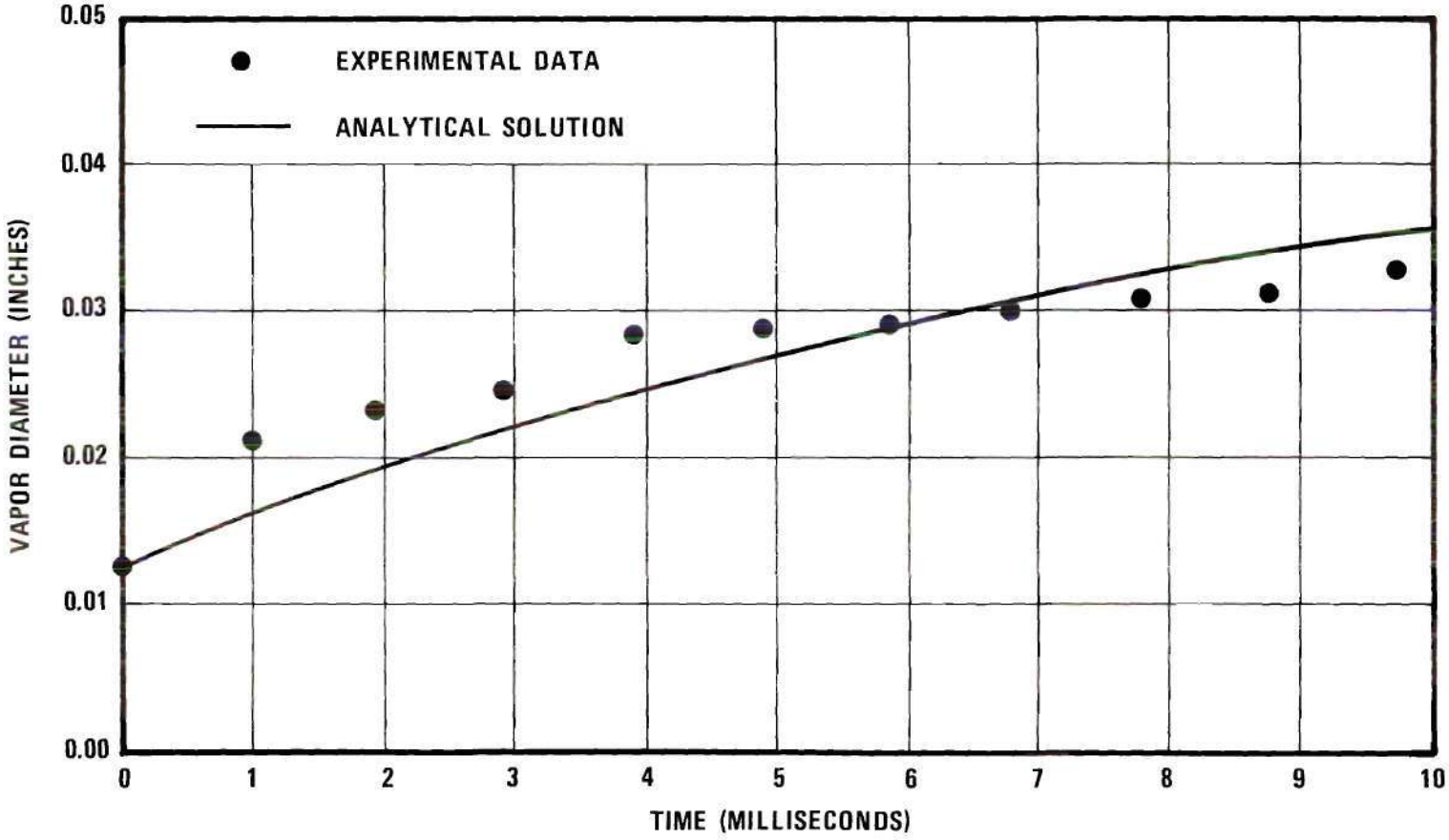


Figure 15. Plot of Vapor Diameter as a Function of Time for Run 23

$T_\infty = 199^\circ F$, $\dot{q} = 0.0136$ Btu/sec.in.

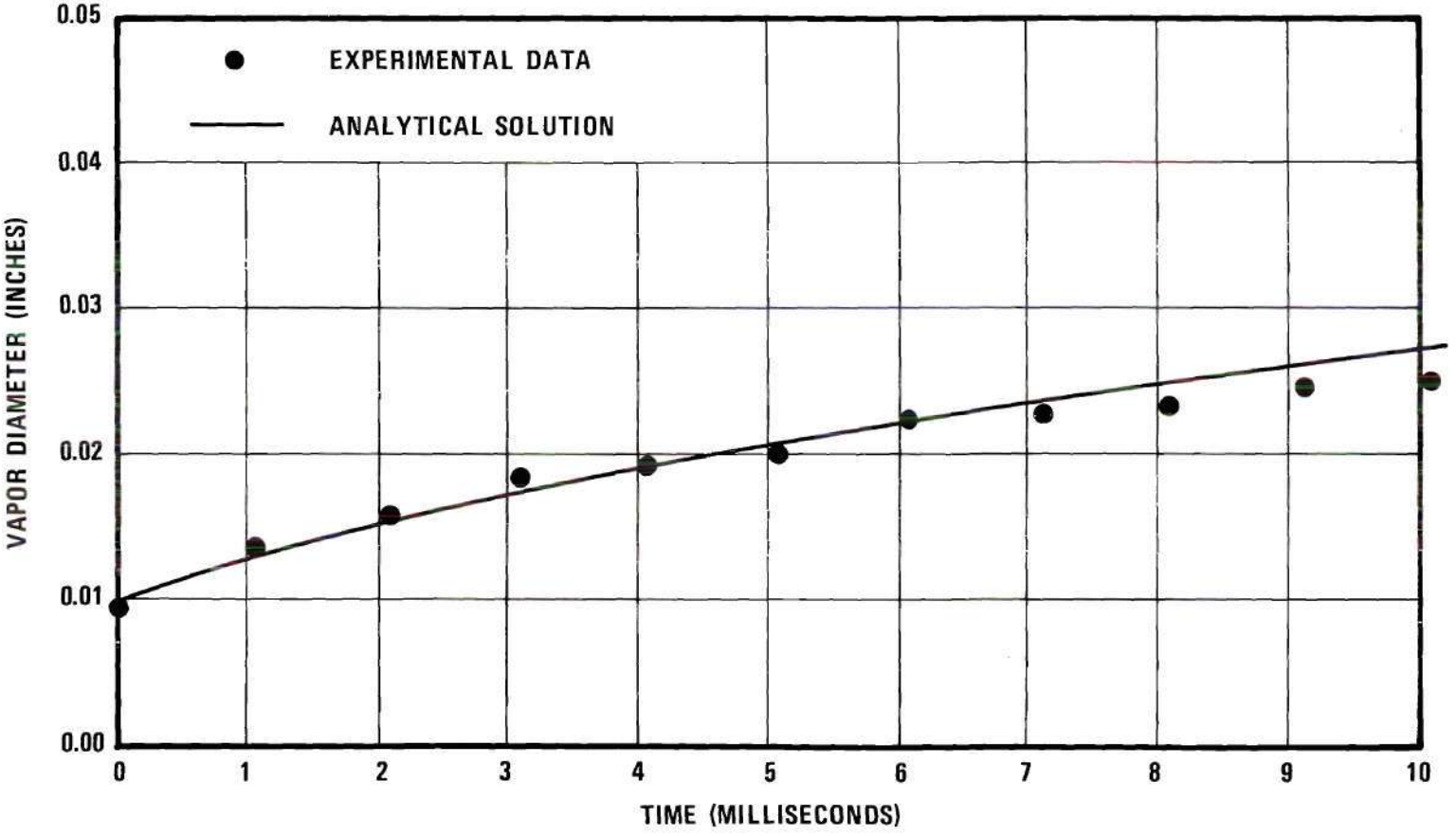


Figure 16. Plot of Vapor Diameter as a Function of Time for Run 27

$T_\infty = 197^\circ F$, $\dot{q} = 0.0204$ Btu/sec.in.

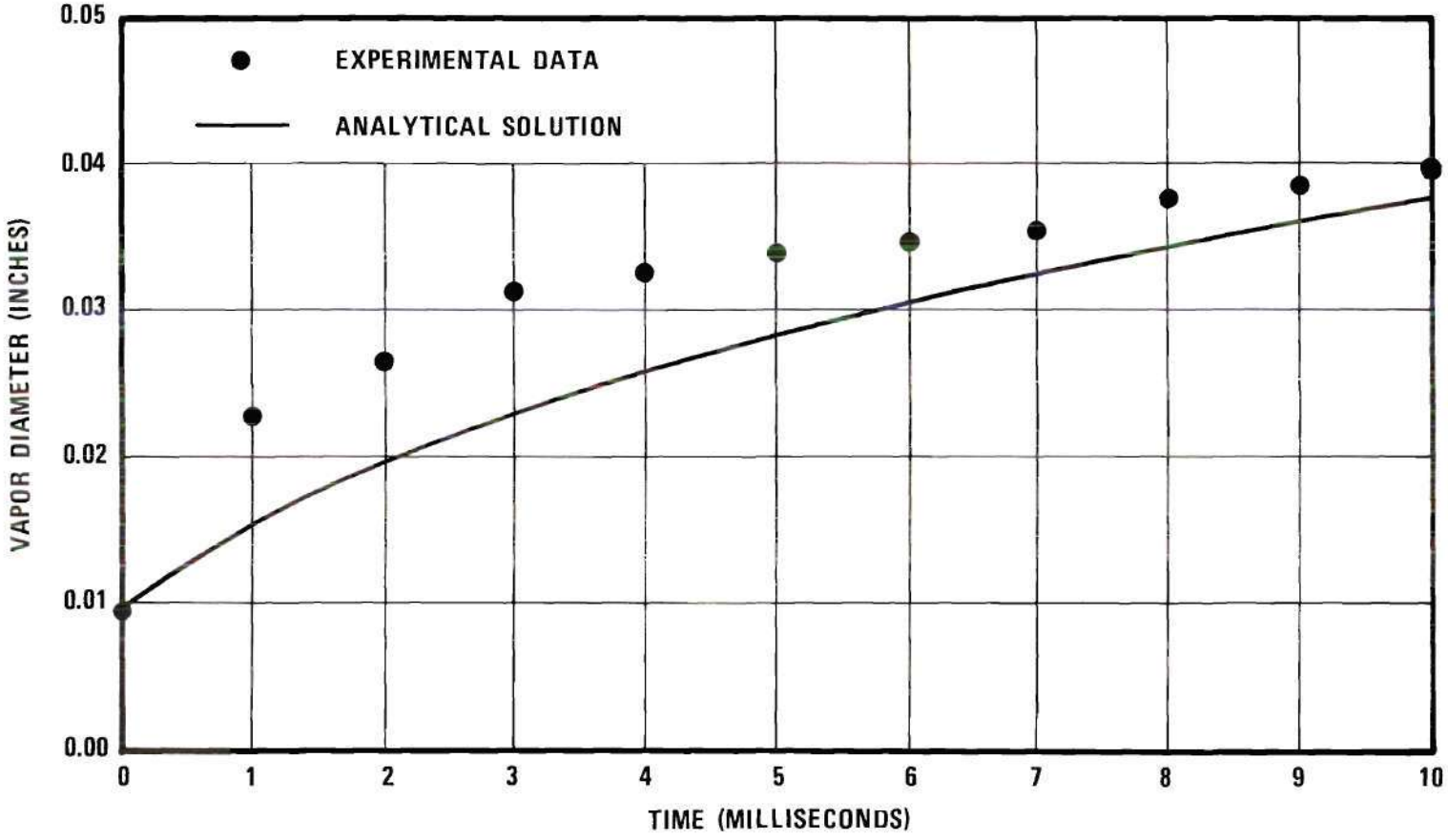


Figure 17. Plot of Vapor Diameter as a Function of Time for Run 29

$T_\infty = 204.5^\circ F$, $\dot{q} = 0.0206$ Btu/sec.in.

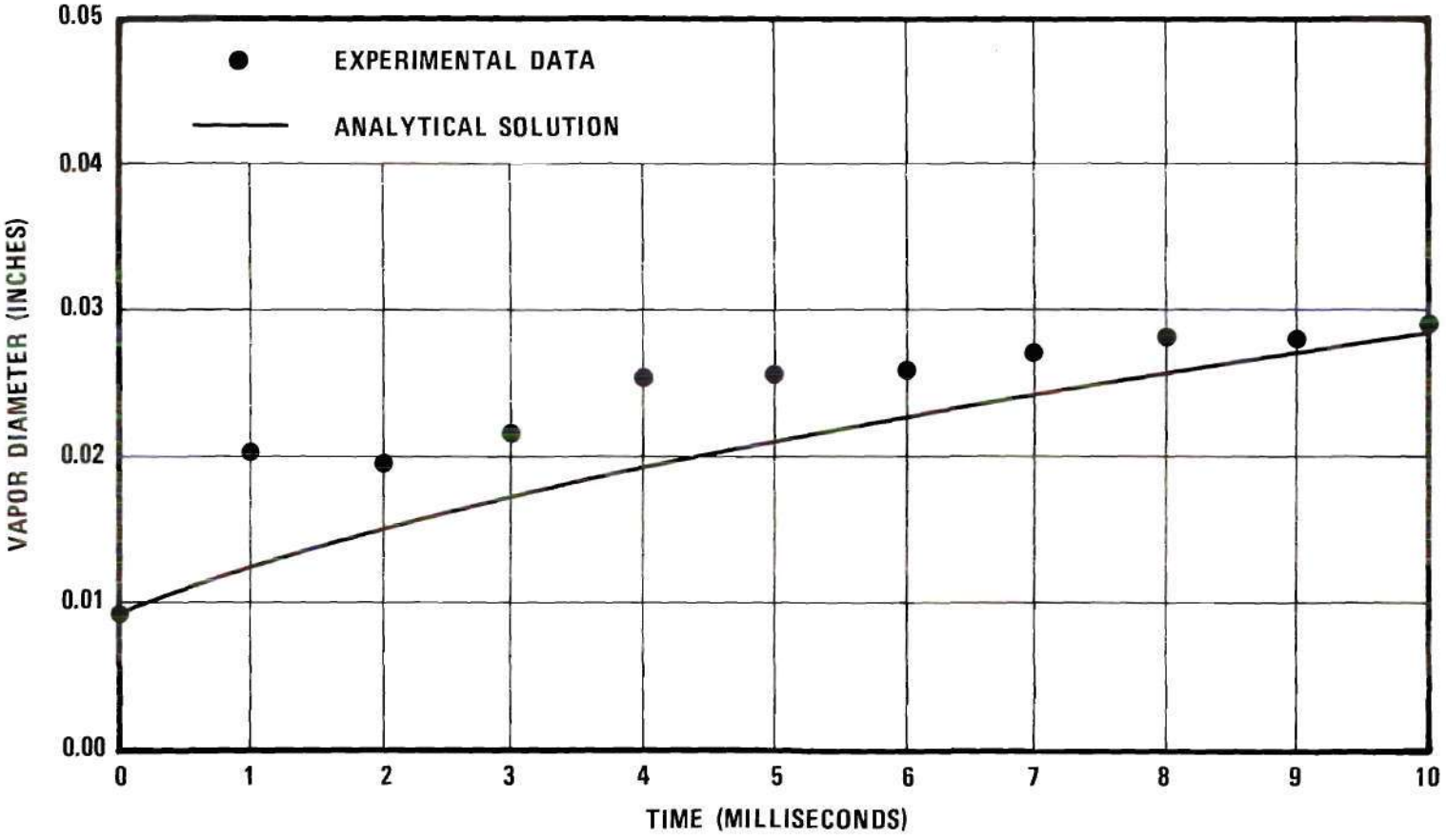


Figure 18. Plot of Vapor Diameter as a Function of Time for Run 30

$T_\infty = 188^\circ F$, $\dot{q} = 0.0179$ Btu/sec.in.

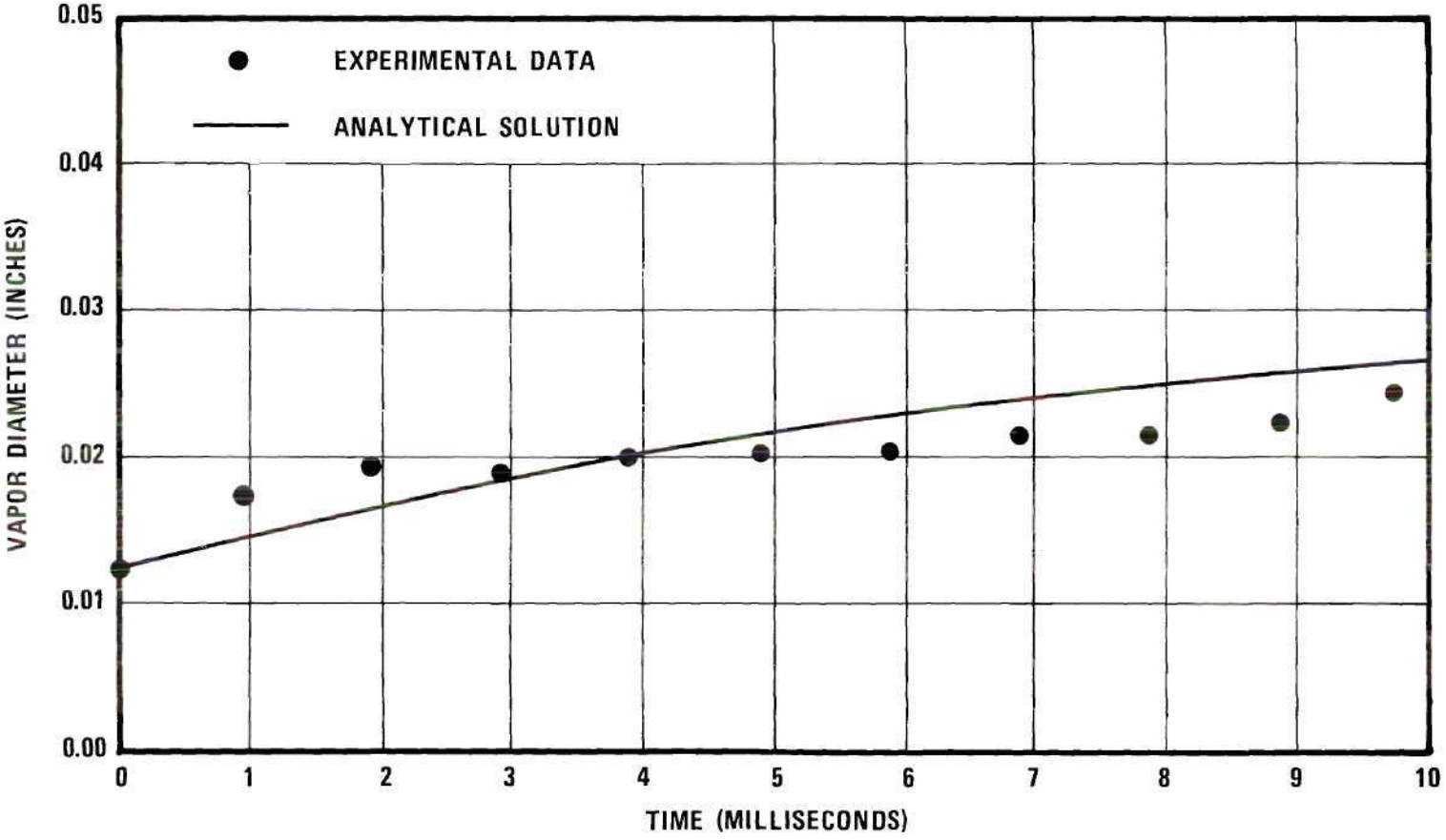


Figure 19. Plot of Vapor Diameter as a Function of Time for Run 32

$T_\infty = 190^\circ F$, $\dot{q} = 0.0406$ Btu/sec.in.

# CHAPTER VI

# CONCLUSIONS AND RECOMMENDATIONS

## Conclusions

The major conclusions drawn from this experimental and analytical investigation may be stated as follows.

1. Vapor film growth in transient film boiling of subcooled water from a small diameter cylindrical surface of low thermal emissivity is primarily controlled by conduction heat transfer within the vapor film and convection heat transfer from the vapor-liquid interface to the subcooled liquid.

2. The minimum wall temperature for formation of a cylindrical growth of vapor in boiling of subcooled water from a small diameter wire is not only dependent on excess temperature ($\Delta T = T_w - T_{sat}$) but also is dependent on the degree of subcooling.

3. Film boiling is preceded by vigorous nucleation for heating surface temperature changes occurring in as short a time span as 50 microseconds; this nucleation has a pronounced effect on the ensuing rate of vapor formation if the bulk fluid temperature is near the saturation condition, but the effect decreases as the degree of subcooling increases.

4. After cylindrical growth reaches maximum size, the onset of large bubble formation at nodes along the wire due to Taylor-Helmholtz instability is apparent.

5. The use of a capacitance discharge into a resistive heating

element is a satisfactory method for accomplishing a step-change input to a surface for heat transfer investigations. Also, the use of a Wheatstone bridge and resistive heater element system for recording transient element temperature is a satisfactory approach.

## Recommendations

Some further work in this area that is considered to be of significant value is:

1. The effect of radiation from a heater element surface of relatively high thermal emissivity should be investigated.

2. The present analysis should be confirmed for other liquids.

3. The present analysis should be confirmed at different pressure levels.

4. An investigation should be made of the region of vigorous nucleation at the onset of film boiling. This investigation should be conducted at nearly saturated bulk fluid temperature.

5. Transient film boiling in a confined field should be investigated. This would be valuable and informative to both academic and practical applications.

# APPENDICES

# APPENDIX A

# SAMPLE CALCULATIONS

## Evaluation of the Incomplete Γ-Function

The definition of the incomplete Γ-function is given by

$$\Gamma(u,w) = \int_{w}^{\infty} e^{-t}\, t^{u-1}\, dt \quad . \tag{A.1}$$

An alternative form of the incomplete Γ-function may be expressed as

$$\Gamma\left(p+1;\ u\sqrt{p+1}\right) = [1-I(u,p)]\ \Gamma(p+1) \tag{A.2}$$

where

$$\Gamma(p+1) = \int_{0}^{\infty} e^{-x}\, x^{p}\, dx \tag{A.3}$$

is a complete Γ-function, and

$$I(u,p) = \frac{\displaystyle\int_{0}^{u\sqrt{p+1}} e^{-x}\, x^{p}\, dx}{\Gamma(p+1)} \quad . \tag{A.4}$$

Derivation of Equation (A.2) can be obtained from Pearson[20]. The function I(u,p) is also tabulated by the same reference.

In the present investigation, the incomplete Γ-function always takes the form of $\Gamma\left(\frac{A}{2},\frac{A}{2}\right)$ ; therefore, the relations between u, p and A are simply obtained as follows:

$$\frac{A}{2} = p + 1 \tag{A.5}$$

$$\frac{A}{2} = u\sqrt{p + 1} \quad . \tag{A.6}$$

Solving Equations (A.5) and (A.6) simultaneously, then

$$p = \frac{A}{2} - 1 \tag{A.7}$$

$$u = \sqrt{\frac{A}{2}} \quad . \tag{A.8}$$

Therefore

$$\Gamma\left(\frac{A}{2}, \frac{A}{2}\right) = \left[1 - I\left(\sqrt{\frac{A}{2}}, \frac{A}{2} - 1\right)\right]\Gamma\left(\frac{A}{2}\right) \quad . \tag{A.9}$$

The value of the incomplete Γ-function in this investigation can be obtained by evaluating Equation (A.9) with a table of the Incomplete Γ-Function[20] in conjunction with a table of the Complete Γ-Function[21].

Solution of the Transcendental Equation for the Phase Growth Constant of Proportionality

The specific example presented here is for run number 23. The parameters for solution of Equation (4.49) are:

$$\alpha_\ell \rho_v h_{fg} = 0.348 \times 10^{-5} \text{ Btu/in. sec.}$$

$$\frac{\alpha_\ell}{\alpha_v} = 7.7 \times 10^{-3}$$

$$K_\ell = 0.0915 \times 10^{-4} \text{ Btu/in. sec. } ^\circ\text{F} \quad .$$

Applying the energy balance at the metal-vapor interface yields

$$\dot{q} = - \pi r_w^2 \rho_w C_{p,w} \frac{dT_w}{dt} \quad . \tag{A.10}$$

Using the properties of platinum with the temperature versus time plot of Figure 9, then

$$\dot{q} = - \pi(0.0063)^2 \times 0.774 \times 0.035 \times (-4 \times 10^3) = 0.0136 \text{ Btu/in. sec.}$$

Substituting the above data into Equation (4.49), then

$$0.348 \times 10^{-5} A = 2.165 \times 10^{-3} e^{-3.85 \times 10^{-3} A} - \frac{1.83 \times 10^{-5} (212 - 199)\left(\frac{A}{2}\right)^{\frac{A}{2}} e^{\frac{-A}{2}}}{\Gamma\left(\frac{A}{2}, \frac{A}{2}\right)} \quad . \tag{A.11}$$

Equation (A.11) may be solved by the trial and error method. Rewrite Equation (A.11) in a residual form and divide by $0.348 \times 10^{-5}$, then

$$\text{Res.} = 6.225 \times 10^2 e^{-3.85 \times 10^{-3} A} - A - \frac{68.3 \left(\frac{A}{2}\right)^{\frac{A}{2}} e^{\frac{-A}{2}}}{\Gamma\left(\frac{A}{2}, \frac{A}{2}\right)} \quad . \tag{A.12}$$

For a trial solution, assume $A = 80$. This yields

$$\text{Res.} = 457 - 80 - \frac{68.3 (40)^{40} e^{-40}}{\Gamma(40, 40)} \quad . \tag{A.13}$$

The third term in the right-hand side of Equation (A.13) may be evaluated as follows.

$$\ell n \frac{68.3\,(40)^{40}\,e^{-40}}{[1 - I(\sqrt{40},39)]\Gamma(40)} = \ell n\, 68.3 + 40\,\ell n\, 40 - 40 - \ell n\, \Gamma(40) - \ell n\,[1 - I(\sqrt{40},39)]. \quad (A.14)$$

The value of Equation (A.14) is found to be 5.86; therefore, the value of the third term in the right-hand side of Equation (A.13) is 350. Substituting this value into Equation (A.13), then

$$\text{Res.} = 457 - 80 - 350 = 27 \quad . \quad (A.15)$$

The positive residual in Equation (A.12) implies that the heat transfer from the vapor phase to the vapor-liquid interface is greater than the sum of energy required for vaporization and the energy conducted into the liquid phase. Consequently, a greater value of A must be assumed. For the second trial solution, assume A = 82. This yields

$$\text{Res.} = 22.$$

For the third trial solution, assume A = 83. This yields

$$\text{Res.} = -40.5 \quad .$$

The residual changes sign between A equals 82 and 83. Consequently, we can conclude that the value of A is greater than 82 but less than 83. Since the value of A used in Equation (4.51) is under the square root sign, the use of the value 82 and 83 will effect the result by no more than 2.5 percent for the first ten milliseconds in this run.

# APPENDIX B

## VAPOR DIAMETER MEASUREMENT ERROR ANALYSIS

The maximum error associated with determination of the arbitrary function $\phi$ is given by

$$\Delta \phi = \sum \frac{\partial \phi}{\partial m_i} \Delta m_i \qquad \text{(B.1)}$$

where the $m_i$ s are the variables of measurement. The variables of measurement of the vapor cylinder diameters are:

1) wire actual diameter

2) wire projected diameter

3) vapor projected diameter

4) definition of vapor-liquid interface

In terms of the variables of measurement, Equation (B.1) becomes

$$\frac{\Delta D}{D} = \frac{\partial D}{\partial d_1} \frac{\Delta d_1}{D} + \frac{\partial D}{\partial d_2} \frac{\Delta d_2}{D} + \frac{\partial D}{\partial d_3} \frac{\Delta d_3}{D} + \frac{\partial D}{\partial d_4} \frac{\Delta d_4}{D} \quad . \qquad \text{(B.2)}$$

The wire diameter was measured with two instruments and for the number 30 wire was found to be 0.0098 ± 0.00005 inch. The bubble diameter measurement is proportional to the wire diameter. Thus, for the smallest projected wire diameter of 0.48 centimeter,

$$\frac{\partial D}{\partial d_1} \frac{\Delta d_1}{D} = \frac{0.48/2.54}{0.0098} \times \frac{0.00005}{0.48/2.54} = 0.0051 \quad . \qquad \text{(B.3)}$$

The projected wire diameter was measured to within 0.025 centimeter, thus for the worst case

$$\frac{\partial D}{\partial d_2} \frac{\Delta d_2}{D} = \frac{0.025/2.54}{0.48/2.54} = 0.0521 \quad . \qquad \text{(B.4)}$$

The average vapor cylinder projected diameter was on the order of 2.5 centimeters. Thus, the error in measurement resulted in

$$\frac{\partial D}{\partial d_3}\frac{\Delta d_3}{D} = \frac{0.025/2.54}{2.5/2.54} = 0.01 \quad . \tag{B.5}$$

The projected vapor-liquid interface was usually defined to within 0.05 centimeter. Thus, for the average diameter

$$\frac{\partial D}{\partial d_4}\frac{\Delta d_4}{D} = \frac{0.05}{2.5} = 0.02 \quad . \tag{B.6}$$

Substitution of Equations (B.3), (B.4), (B.5), and (B.6) into Equation (B.2), gives the maximum percent error in the vapor cylinder median diameter

$$\frac{\Delta D}{D} = 0.0051 + 0.0521 + 0.01 + 0.02 = 0.0872 \quad , \tag{B.7}$$

or, approximately 9 percent.

If a normal (Gaussian) distribution of errors is assumed, then the probable error becomes

$$\frac{\Delta D}{D}_p = \left[\left(\frac{\partial D}{\partial d_1}\frac{\Delta d_1}{D}\right)^2 + \left(\frac{\partial D}{\partial d_2}\frac{\Delta d_2}{D}\right)^2 + \left(\frac{\partial D}{\partial d_3}\frac{\Delta d_3}{D}\right)^2 + \left(\frac{\partial D}{\partial d_4}\frac{\Delta d_4}{D}\right)^2\right]^{\frac{1}{2}} \quad . \tag{B.8}$$

Substituting Equations (B.3), (B.4), (B.5), and (B.6) into Equation (B.8), we obtain

$$\frac{\Delta D}{D}_p = \left[(0.0051)^2 + (0.0521)^2 + (0.01)^2 + (0.02)^2\right]^{\frac{1}{2}} = 0.0572. \tag{B.9}$$

or, approximately 6 percent.

# APPENDIX C

CALIBRATION AND DESCRIPTIVE DATA FOR HEATER ELEMENTS

GENERAL TEST DATA FOR EACH TRANSIENT BOILING EXPERIMENT

VAPOR GROWTH RATE DATA

Table 2. Temperature Calibration Data for All Heater Elements

| Element | Date | Thermocouple EMF Millivolts | Bridge Unbalance Millivolts | Bridge Current Milliamps |
|---|---|---|---|---|
| A | 4-29-67 | 0.3188 | 1.08 | 80 |
| A | 4-29-67 | 1.5122 | 4.00 | 80 |
| A | 4-29-67 | 2.3940 | 5.75 | 80 |
| A | 4-29-67 | 4.0070 | 8.76 | 80 |
| A | 4-29-67 | 5.2672 | 10.88 | 80 |
| A | 4-29-67 | 6.3301 | 12.52 | 80 |
| B | 8-18-67 | 0.1410 | 0.20 | 80 |
| B | 8-18-67 | 1.0735 | 2.40 | 80 |
| B | 8-18-67 | 2.0395 | 4.10 | 80 |
| B | 8-18-67 | 2.9040 | 5.50 | 80 |
| B | 8-18-67 | 3.8960 | 6.96 | 80 |
| B | 8-18-67 | 4.9575 | 8.30 | 80 |
| B | 8-18-67 | 5.9135 | 9.66 | 80 |
| B | 8-18-67 | 6.9205 | 11.10 | 80 |
| B | 8-18-67 | 7.8890 | 12.34 | 80 |
| C | 8-29-67 | 0.1360 | 0.20 | 120 |
| C | 8-29-67 | 1.1323 | 2.16 | 120 |
| C | 8-29-67 | 2.0250 | 3.20 | 120 |
| C | 8-29-67 | 2.9451 | 5.00 | 120 |
| C | 8-29-67 | 3.8866 | 6.20 | 120 |
| C | 8-29-67 | 4.8785 | 7.40 | 120 |
| C | 8-29-67 | 5.9425 | 8.60 | 120 |
| C | 8-29-67 | 6.9125 | 9.80 | 120 |
| C | 8-29-67 | 7.8683 | 10.90 | 120 |
| D | 9-18-67 | 0.1335 | 0.35 | 120 |
| D | 9-18-67 | 1.2070 | 1.50 | 120 |
| D | 9-18-67 | 2.4231 | 4.44 | 120 |
| D | 9-18-67 | 3.8550 | 6.40 | 120 |
| D | 9-18-67 | 5.6290 | 8.70 | 120 |
| D | 9-18-67 | 6.9930 | 10.36 | 120 |
| E | 9-21-67 | 0.1335 | 0.80 | 50 |
| E | 9-21-67 | 1.515 | 3.80 | 50 |

(continued)

Table 2. (Continued)

| Element | Date | Thermocouple EMF Millivolts | Bridge Unbalance Millivolts | Bridge Current Milliamps |
|---|---|---|---|---|
| | | (continued) | | |
| E | 9-21-67 | 3.1105 | 6.50 | 50 |
| E | 9-21-67 | 5.500 | 10.00 | 50 |
| E | 9-21-67 | 6.5451 | 11.26 | 50 |
| E | 9-21-67 | 7.3450 | 12.36 | 50 |
| F | 9-26-67 | 0.1350 | 1.10 | 50 |
| F | 9-26-67 | 1.7581 | 4.60 | 50 |
| F | 9-26-67 | 3.1050 | 6.86 | 50 |
| F | 9-26-67 | 4.4750 | 9.04 | 50 |
| F | 9-26-67 | 5.9450 | 11.16 | 50 |
| F | 9-26-67 | 7.4550 | 13.10 | 50 |
| F | 9-26-67 | 8.9800 | 15.00 | 50 |
| G | 9-28-67 | 0.5650 | 1.90 | 100 |
| G | 9-28-67 | 1.7510 | 3.55 | 100 |
| G | 9-28-67 | 3.0200 | 5.10 | 100 |
| G | 9-28-67 | 4.4500 | 6.80 | 100 |
| G | 9-28-67 | 5.8951 | 8.16 | 100 |
| G | 9-28-67 | 7.480 | 9.50 | 100 |

Table 3. Heater Element Descriptive Data

| Element | Description |
|---|---|
| A | Number 30 (0.0098 inch) diameter, commercially pure platinum wire, 2.00 inches long. |
| B | Number 30 (0.0098 inch) diameter, commercially pure platinum wire, 1.91 inches long. |
| C | Number 28 (0.0126 inch) diameter, commercially pure platinum wire, 1.94 inches long. |
| D | Number 28 (0.0126 inch) diameter, commercially pure platinum wire, 1.94 inches long. |
| E | Number 30 (0.0098 inch) diameter, commercially pure platinum wire, 2.19 inches long. |
| F | Number 30 (0.0098 inch) diameter, commercially pure platinum wire, 2.19 inches long. |
| G | Number 28 (0.0126 inch) diameter, commercially pure platinum wire, 1.94 inches long. |

Table 4. General Data for Transient Boiling Tests

| Run No. | Bulk Water Temperature (°F) | Water Depth (in.) | Film Type | Lens f/stop | Data Ext. Tube (in.) | Barometric Pressure (in.Hg.) |
|---|---|---|---|---|---|---|
| 8 | 194 | 1.50 | Dupont 931A | 1.4 | 0.5 | 29.36 |
| 18 | 203 | 2.00 | Dupont 931A | 1.4 | 1.0 | 29.37 |
| 19 | 202.5 | 1.80 | Dupont 931A | 1.4 | 1.0 | 29.25 |
| 20 | 205 | 1.80 | Dupont 931A | 1.4 | 1.0 | 29.25 |
| 21 | 192 | 2.00 | Dupont 931A | 1.4 | 1.0 | 29.22 |
| 23 | 199 | 1.80 | Dupont 931A | 1.4 | 1.0 | 29.36 |
| 27 | 197 | 2.00 | Dupont 931A | 1.4 | 1.0 | 29.31 |
| 29 | 204.5 | 2.30 | Kodak Tri-X | 1.4 | 1.0 | 29.24 |
| 30 | 188 | 2.20 | Kodak Tri-X | 1.4 | 1.0 | 29.24 |
| 32 | 190 | 2.10 | Kodak Tri-X | 1.4 | 1.0 | 28.81 |

Table 5. Heater Element Temperature Data for Transient Boiling Tests

| Run No. | Element | Time Milliseconds | 1 | 2 | 3 | 4 | 5 | 6 | 7 | 8 | 9 | 10 |
|---|---|---|---|---|---|---|---|---|---|---|---|---|
| 8 | A | | 13.60 | 14.60 | 14.56 | 14.50 | 14.44 | 14.36 | 14.30 | 14.24 | 14.18 | 14.12 |
| 18 | B | | 13.08 | 12.98 | 12.90 | 12.80 | 12.70 | 12.60 | 12.54 | 12.40 | 12.35 | 12.30 |
| 19 | C | | ----- | ----- | 8.46 | 8.94 | 8.90 | 8.86 | 8.82 | 8.76 | 8.70 | 8.66 |
| 20 | C | | ----- | ----- | 9.24 | 9.20 | 9.16 | 9.12 | 9.08 | 9.06 | 9.04 | 9.00 |
| 21 | D | | ----- | 8.50 | 10.00 | 10.60 | 10.50 | 10.40 | 10.30 | 10.20 | 10.10 | 10.00 |
| 23 | D | | 10.40 | 10.44 | 10.50 | 10.48 | 10.46 | 10.44 | 10.42 | 10.40 | 10.36 | 10.34 |
| 27 | E | | | 15.10 | | 14.96 | | 14.84 | | 14.70 | | 14.60 |
| 29 | F | | 16.10 | 16.30 | 16.10 | 16.05 | 16.00 | 15.95 | 15.90 | 15.85 | 15.80 | 15.75 |
| 30 | F | | 15.35 | 15.70 | 15.65 | 15.60 | 15.55 | 15.50 | 15.45 | 15.40 | 15.35 | 15.30 |
| 32 | G | | | 10.50 | | 10.36 | | 10.20 | | 10.06 | | 9.90 |

Table 6. Film Growth Rate Data for Run Number 8

| Frame No. | Frame Station | Vapor Bubble Projected Diameter - Centimeters | | | | | | | | | | | |
|---|---|---|---|---|---|---|---|---|---|---|---|---|---|
| | | 1 | 2 | 3 | 4 | 5 | 6 | 7 | 8 | 9 | 10 | 11 | 12 |
| | | 13 | 14 | 15 | 16 | 17 | 18 | 19 | 20 | 21 | 22 | 23 | 24 |
| wire | | 0.60 | 0.60 | 0.55 | 0.50 | 0.50 | 0.50 | 0.50 | 0.50 | 0.48 | 0.50 | 0.50 | 0.48 |
| | | 0.50 | 0.50 | 0.50 | | | | | | | | | |
| 4 | | 1.15 | 0.90 | 0.80 | 0.62 | 0.70 | 0.60 | 0.75 | 0.80 | 0.95 | 0.75 | 0.70 | 0.75 |
| | | 0.90 | 0.60 | 0.65 | 0.80 | 0.80 | 0.70 | 0.65 | 0.85 | 0.80 | 1.00 | 0.85 | 0.65 |
| 8 | | 1.10 | 0.80 | 1.15 | 0.80 | 1.00 | 0.75 | 1.00 | 1.00 | 0.70 | 0.85 | 1.20 | 0.90 |
| | | 0.95 | 0.70 | 0.75 | 0.95 | 0.70 | 0.65 | 0.70 | 0.90 | 0.90 | 1.10 | 1.05 | 0.80 |
| 12 | | 1.20 | 1.05 | 1.20 | 0.80 | 1.15 | 0.95 | 1.30 | 1.15 | 0.90 | 0.85 | 1.25 | 1.20 |
| | | 1.05 | 0.65 | 0.75 | 1.35 | 0.90 | 0.80 | 0.85 | 0.80 | 0.70 | 1.40 | 1.35 | 0.85 |
| 16 | | 1.55 | 1.00 | 0.85 | 1.25 | 0.75 | 0.80 | 1.05 | 1.35 | 1.75 | 0.75 | 0.70 | 1.50 |
| | | 1.25 | 1.00 | 0.65 | 0.60 | 1.50 | 1.25 | 0.90 | 1.30 | 1.00 | 0.60 | 1.45 | 1.35 |
| 20 | | 1.05 | 1.70 | 1.65 | 0.80 | 0.85 | 0.70 | 1.70 | 1.00 | 0.85 | 0.60 | 1.15 | 1.80 |
| | | 0.80 | 1.15 | 0.65 | 1.00 | 1.90 | 1.05 | 1.50 | 0.70 | 0.80 | 1.75 | 1.15 | 0.90 |
| 24 | | 1.95 | 0.90 | 1.30 | 1.25 | 0.85 | 1.05 | 0.90 | 1.70 | 1.95 | 0.70 | 0.65 | 1.35 |
| | | 2.00 | 1.15 | 0.90 | 0.65 | 1.30 | 1.70 | 0.85 | 1.05 | 1.15 | 0.70 | 1.40 | 1.10 |
| 28 | | 1.15 | 1.80 | 1.90 | 0.85 | 1.10 | 0.85 | 1.70 | 0.90 | 0.85 | 0.90 | 0.80 | 1.75 |
| | | 0.70 | 1.45 | 1.00 | 0.75 | 1.85 | 1.70 | 0.75 | 0.85 | 0.90 | 1.90 | 1.50 | 1.00 |

(continued)

Table 6. (Continued)

| Frame No. | Frame Station | Vapor Bubble Projected Diameter - Centimeters | | | | | | | | | | | |
|---|---|---|---|---|---|---|---|---|---|---|---|---|---|
| | | 1 | 2 | 3 | 4 | 5 | 6 | 7 | 8 | 9 | 10 | 11 | 12 |
| | | 13 | 14 | 15 | 16 | 17 | 18 | 19 | 20 | 21 | 22 | 23 | 24 |
| 32 | | 1.15 | 1.90 | 1.80 | 0.80 | 0.90 | 2.00 | 1.80 | 1.25 | 0.85 | 1.50 | 1.55 | 1.55 |
| | | 0.80 | 1.00 | 0.75 | 0.90 | 1.20 | 1.75 | 0.70 | 0.90 | 1.20 | 1.80 | 1.30 | 1.00 |
| 36 | | 1.20 | 1.35 | 1.20 | 0.60 | 0.80 | 1.75 | 2.15 | 0.70 | 0.80 | 1.15 | 1.85 | 1.65 |
| | | 1.20 | 1.15 | 0.70 | 0.75 | 1.15 | 2.20 | 0.80 | 1.10 | 1.00 | 2.35 | 1.10 | 1.00 |
| 40 | | 1.15 | 1.70 | 1.60 | 0.80 | 0.90 | 1.60 | 1.90 | 0.85 | 0.90 | 0.70 | 2.05 | 1.80 |
| | | 1.20 | 0.85 | 0.70 | 0.95 | 1.00 | 1.95 | 1.45 | 0.90 | 1.50 | 2.40 | 0.90 | 1.20 |

Framing Speed: 40 frames = 10 milliseconds

Table 7. Film Growth Rate Data for Run Number 18

| Frame No. | Frame Station | Vapor Bubble Projected Diameter - Centimeters | | | | | | | | | | | |
|---|---|---|---|---|---|---|---|---|---|---|---|---|---|
| | | 1 | 2 | 3 | 4 | 5 | 6 | 7 | 8 | 9 | 10 | 11 | 12 |
| | | 13 | 14 | 15 | 16 | 17 | 18 | 19 | 20 | 21 | 22 | 23 | 24 |
| wire | | 0.60 | 0.55 | 0.60 | 0.60 | 0.60 | 0.60 | 0.58 | 0.60 | 0.60 | 0.63 | | |
| 4 | | 1.55 | 1.20 | 1.30 | 1.60 | 2.20 | 1.60 | 1.75 | 1.70 | 1.20 | 1.30 | 1.00 | 1.55 |
| | | 2.00 | 0.90 | 1.40 | 1.45 | 1.60 | 1.30 | 1.70 | 1.50 | 1.90 | 1.70 | 1.50 | 1.70 |
| 8 | | 1.85 | 1.90 | 1.70 | 1.50 | 1.70 | 2.00 | 2.10 | 1.10 | 1.30 | 1.50 | 1.60 | 1.60 |
| | | 1.50 | 1.20 | 0.95 | 1.25 | 1.70 | 1.00 | 1.50 | 1.40 | 1.90 | 1.70 | 1.80 | 1.75 |
| 12 | | 2.30 | 2.80 | 1.10 | 0.90 | 1.20 | 2.85 | 2.75 | 1.00 | 1.70 | 1.00 | 1.00 | 2.75 |
| | | 2.40 | 1.00 | 1.40 | 1.00 | 1.85 | 2.60 | 1.70 | 1.50 | 2.20 | 2.05 | 1.20 | 1.00 |
| 16 | | 2.40 | 2.55 | 1.40 | 1.00 | 2.00 | 3.15 | 1.20 | 1.20 | 1.10 | 1.10 | 2.15 | 2.40 |
| | | 1.10 | 1.00 | 0.80 | 1.20 | 2.60 | 2.10 | 1.50 | 2.50 | 2.00 | 1.30 | 1.30 | 2.10 |
| 20 | | 2.05 | 2.30 | 1.90 | 1.50 | 2.20 | 2.60 | 1.60 | 1.20 | 1.20 | 1.45 | 2.00 | 2.10 |
| | | 1.30 | 0.90 | 1.20 | 2.00 | 2.50 | 1.30 | 1.70 | 2.00 | 2.25 | 1.95 | 1.72 | 2.00 |
| 24 | | 2.60 | 2.70 | 1.10 | 1.30 | 2.80 | 3.10 | 1.05 | 1.55 | 1.45 | 1.10 | 2.30 | 2.00 |
| | | 1.10 | 1.50 | 1.00 | 1.20 | 2.55 | 1.60 | 2.00 | 2.60 | 1.70 | 1.05 | 1.30 | 2.55 |
| 28 | | 2.80 | 2.90 | 1.60 | 1.00 | 3.20 | 3.15 | 1.90 | 1.50 | 1.30 | 1.10 | 3.10 | 2.40 |
| | | 0.80 | 1.10 | 1.00 | 2.15 | 2.80 | 2.70 | 2.60 | 2.70 | 1.50 | 1.40 | 1.10 | 3.10 |

(continued)

Table 7. (Continued)

| Frame No. | Frame Station | Vapor Bubble Projected Diameter - Centimeters | | | | | | | | | | | |
|---|---|---|---|---|---|---|---|---|---|---|---|---|---|
| | | 1 | 2 | 3 | 4 | 5 | 6 | 7 | 8 | 9 | 10 | 11 | 12 |
| | | 13 | 14 | 15 | 16 | 17 | 18 | 19 | 20 | 21 | 22 | 23 | 24 |
| 32 | | 2.50 | 2.45 | 2.30 | 1.60 | 1.70 | 3.30 | 3.10 | 3.30 | 1.30 | 0.90 | 2.10 | 2.70 |
| | | 2.30 | 1.60 | 0.80 | 1.26 | 1.05 | 2.25 | 3.55 | 3.60 | 2.30 | 1.30 | 1.75 | 3.10 |
| 36 | | 3.10 | 3.00 | 2.50 | 1.90 | 1.60 | 3.15 | 2.65 | 3.20 | 2.20 | 0.85 | 2.15 | 2.00 |
| | | 2.90 | 2.80 | 1.70 | 1.00 | 1.75 | 2.20 | 2.10 | 3.40 | 4.40 | 1.00 | 1.00 | 1.50 |
| 40 | | 2.20 | 2.90 | 2.75 | 1.20 | 1.50 | 2.80 | 3.20 | 3.25 | 2.10 | 1.50 | 1.85 | 2.80 |
| | | 2.75 | 1.10 | 1.70 | 1.00 | 1.60 | 2.55 | 3.50 | 3.10 | 2.40 | 1.70 | 1.30 | 3.30 |

Framing Speed: 59 frames = 15 milliseconds

Table 8. Film Growth Rate Data for Run Number 19

| Frame No. | Frame Station | Vapor Bubble Projected Diameter - Centimeters | | | | | | | | | | | |
|---|---|---|---|---|---|---|---|---|---|---|---|---|---|
| | | 1 | 2 | 3 | 4 | 5 | 6 | 7 | 8 | 9 | 10 | 11 | 12 |
| | | 13 | 14 | 15 | 16 | 17 | 18 | 19 | 20 | 21 | 22 | 23 | 24 |
| wire | | 0.80 | 0.80 | 0.70 | 0.80 | 0.75 | 0.75 | 0.75 | 0.75 | 0.70 | 0.70 | 0.70 | 0.70 |
| 4 | | 1.50 | 1.40 | 1.30 | 1.90 | 2.30 | 2.30 | 1.15 | 1.20 | 1.35 | 1.00 | 2.20 | 2.40 |
| | | 1.10 | 1.00 | 1.10 | 1.20 | 1.80 | 1.70 | 2.25 | 1.70 | 1.00 | 1.50 | 1.40 | 1.20 |
| 8 | | 1.85 | 1.35 | 1.20 | 1.10 | 1.15 | 1.60 | 1.80 | 1.35 | 1.35 | 1.90 | 1.80 | 1.60 |
| | | 1.50 | 1.50 | 1.10 | 0.80 | 0.80 | 1.00 | 1.70 | 2.35 | 1.70 | 1.50 | 1.45 | 1.80 |
| 12 | | 2.00 | 1.20 | 1.00 | 1.30 | 1.60 | 1.95 | 2.00 | 1.80 | 1.50 | 1.50 | 2.00 | 1.90 |
| | | 1.50 | 1.90 | 1.30 | 1.20 | 1.10 | 1.20 | 2.10 | 2.20 | 1.50 | 1.10 | 1.20 | 1.20 |
| 16 | | 1.65 | 1.30 | 1.20 | 1.20 | 2.40 | 2.00 | 1.30 | 1.15 | 1.10 | 1.10 | 2.00 | 2.50 |
| | | 1.50 | 1.10 | 1.20 | 1.20 | 1.30 | 2.20 | 1.90 | 1.50 | 1.30 | 2.00 | 1.50 | 1.40 |
| 20 | | 2.10 | 2.20 | 1.30 | 1.00 | 1.20 | 1.30 | 1.60 | 1.95 | 1.30 | 1.35 | 1.40 | 2.00 |
| | | 1.80 | 1.90 | 2.00 | 1.30 | 1.00 | 1.00 | 1.60 | 2.40 | 2.50 | 2.30 | 1.00 | 1.10 |
| 24 | | 2.00 | 1.50 | 1.60 | 1.00 | 1.60 | 1.80 | 2.00 | 1.30 | 1.55 | 1.85 | 1.75 | 2.10 |
| | | 1.80 | 1.80 | 1.90 | 1.35 | 1.20 | 1.35 | 2.80 | 2.10 | 1.20 | 1.60 | 1.90 | 1.80 |
| 28 | | 2.30 | 2.00 | 1.20 | 1.25 | 1.30 | 1.60 | 2.05 | 2.00 | 1.75 | 1.65 | 1.10 | 1.50 |
| | | 2.90 | 2.40 | 1.00 | 1.10 | 1.25 | 0.90 | 1.55 | 2.70 | 2.90 | 2.00 | 1.00 | 1.35 |

(continued)

Table 8. (Continued)

| Frame No. | Frame Station | Vapor Bubble Projected Diameter - Centimeters | | | | | | | | | | | |
|---|---|---|---|---|---|---|---|---|---|---|---|---|---|
| | | 1 | 2 | 3 | 4 | 5 | 6 | 7 | 8 | 9 | 10 | 11 | 12 |
| | | 13 | 14 | 15 | 16 | 17 | 18 | 19 | 20 | 21 | 22 | 23 | 24 |
| 32 | | 2.60 | 1.95 | 1.00 | 0.90 | 1.30 | 1.30 | 2.10 | 2.50 | 2.00 | 1.20 | 1.10 | 2.00 |
| | | 2.70 | 2.90 | 1.80 | 0.90 | 1.00 | 0.90 | 1.50 | 2.50 | 3.10 | 2.40 | 1.20 | 1.30 |
| 36 | | 2.30 | 1.40 | 1.15 | 1.35 | 1.60 | 2.05 | 2.00 | 1.90 | 1.30 | 1.50 | 2.00 | 2.80 |
| | | 2.90 | 1.80 | 1.20 | 1.15 | 1.05 | 1.40 | 2.90 | 3.00 | 2.70 | 1.00 | 1.20 | 2.40 |
| 40 | | 2.70 | 1.30 | 1.20 | 1.25 | 1.30 | 1.50 | 2.90 | 3.20 | 1.70 | 1.35 | 1.25 | 2.35 |
| | | 3.50 | 2.70 | 1.60 | 1.50 | 1.20 | 1.10 | 1.90 | 3.10 | 2.70 | 2.40 | 1.10 | 1.20 |

Framing Speed: 32 frames = 8 milliseconds

Table 9. Film Growth Rate Data for Run Number 20

| Frame No. | Frame Station | Vapor Bubble Projected Diameter - Centimeters | | | | | | | | | | | |
|---|---|---|---|---|---|---|---|---|---|---|---|---|---|
| | | 1 | 2 | 3 | 4 | 5 | 6 | 7 | 8 | 9 | 10 | 11 | 12 |
| | | 13 | 14 | 15 | 16 | 17 | 18 | 19 | 20 | 21 | 22 | 23 | 24 |
| wire | | 0.75 | 0.80 | 0.80 | 0.85 | 0.80 | 0.80 | 0.80 | 0.75 | 0.75 | 0.80 | 0.80 | 0.80 |
| 4 | | 1.50 | 1.35 | 1.50 | 2.70 | 2.50 | 1.80 | 1.35 | 1.60 | 1.50 | 1.80 | 2.60 | 2.00 |
| | | 1.30 | 1.25 | 1.00 | 1.00 | 2.20 | 3.00 | 2.50 | 1.20 | 1.20 | 1.30 | 1.05 | 1.30 |
| 8 | | 1.70 | 1.20 | 2.15 | 2.50 | 2.40 | 1.60 | 1.50 | 1.50 | 1.25 | 2.10 | 2.40 | 2.30 |
| | | 1.30 | 1.20 | 1.00 | 1.60 | 2.50 | 2.70 | 2.10 | 1.50 | 1.30 | 1.50 | 2.00 | 2.10 |
| 12 | | 1.30 | 1.50 | 1.80 | 2.50 | 2.60 | 1.90 | 1.35 | 1.15 | 1.10 | 1.35 | 3.20 | 2.30 |
| | | 1.70 | 1.30 | 1.30 | 1.50 | 2.40 | 2.80 | 2.50 | 1.70 | 1.50 | 1.60 | 1.50 | 1.50 |
| 16 | | 1.50 | 1.60 | 2.20 | 2.70 | 2.60 | 2.30 | 1.40 | 1.50 | 1.90 | 1.90 | 2.40 | 2.55 |
| | | 1.50 | 1.90 | 1.00 | 1.30 | 2.30 | 3.20 | 1.30 | 1.20 | 2.30 | 2.20 | 1.50 | 1.60 |
| 20 | | 1.40 | 2.10 | 2.80 | 3.00 | 2.20 | 1.50 | 1.30 | 1.30 | 2.50 | 3.30 | 2.80 | 1.00 |
| | | 0.90 | 1.00 | 1.40 | 2.50 | 2.50 | 2.30 | 2.10 | 1.90 | 1.20 | 1.00 | 1.00 | 1.50 |
| 24 | | 1.70 | 1.60 | 2.20 | 2.70 | 2.60 | 2.30 | 1.40 | 1.50 | 1.90 | 1.90 | 2.40 | 2.55 |
| | | 1.40 | 1.90 | 1.00 | 1.30 | 2.30 | 3.20 | 1.30 | 1.20 | 2.30 | 2.20 | 1.50 | 1.60 |
| 28 | | 1.50 | 2.50 | 2.70 | 2.70 | 2.30 | 1.10 | 1.15 | 2.30 | 2.70 | 2.70 | 2.65 | 1.50 |
| | | 1.00 | 0.80 | 1.50 | 2.20 | 2.10 | 1.90 | 2.00 | 2.30 | 2.00 | 1.20 | 1.50 | 2.60 |

(continued)

Table 9. (Continued)

| Frame No. | Frame Station | Vapor Bubble Projected Diameter - Centimeters | | | | | | | | | | | |
|---|---|---|---|---|---|---|---|---|---|---|---|---|---|
| | | 1 | 2 | 3 | 4 | 5 | 6 | 7 | 8 | 9 | 10 | 11 | 12 |
| | | 13 | 14 | 15 | 16 | 17 | 18 | 19 | 20 | 21 | 22 | 23 | 24 |
| 32 | | 1.80 | 1.55 | 2.80 | 3.55 | 3.20 | 1.20 | 1.55 | 1.30 | 2.20 | 2.50 | 2.30 | 2.25 |
| | | 2.05 | 1.20 | 1.10 | 1.00 | 3.00 | 2.50 | 1.50 | 1.20 | 1.25 | 2.00 | 2.00 | 1.50 |
| 36 | | 1.40 | 1.90 | 3.25 | 3.20 | 3.40 | 2.30 | 1.45 | 1.30 | 1.50 | 3.00 | 2.90 | 2.80 |
| | | 1.30 | 1.40 | 1.30 | 1.70 | 2.80 | 3.00 | 2.60 | 1.70 | 1.60 | 2.70 | 1.80 | 2.50 |
| 40 | | 2.10 | 2.00 | 2.50 | 3.70 | 2.90 | 2.00 | 1.00 | 1.00 | 1.60 | 3.00 | 2.80 | 2.40 |
| | | 1.10 | 0.95 | 1.00 | 1.80 | 2.00 | 3.10 | 1.60 | 1.00 | 1.90 | 2.50 | 2.20 | 1.60 |

Framing Speed: 41 frames = 10 milliseconds

Table 10. Film Growth Rate Data for Run Number 21

| Frame No. | Frame Station | Vapor Bubble Projected Diameter - Centimeters | | | | | | | | | | | |
|---|---|---|---|---|---|---|---|---|---|---|---|---|---|
| | | 1 | 2 | 3 | 4 | 5 | 6 | 7 | 8 | 9 | 10 | 11 | 12 |
| | | 13 | 14 | 15 | 16 | 17 | 18 | 19 | 20 | 21 | 22 | 23 | 24 |
| wire | | 0.65 | 0.60 | 0.60 | 0.60 | 0.60 | 0.60 | 0.60 | 0.60 | 0.60 | 0.65 | 0.60 | |
| 4 | | 1.05 | 0.90 | 1.00 | 0.85 | 1.00 | 0.80 | 0.90 | 0.75 | 0.85 | 0.90 | 1.00 | 1.05 |
| | | 1.05 | 1.00 | 1.00 | 0.90 | 1.00 | 0.95 | 1.00 | 0.90 | 0.90 | 0.95 | 0.80 | 0.70 |
| 8 | | 1.20 | 1.25 | 1.10 | 1.10 | 1.10 | 1.05 | 1.00 | 1.05 | 1.00 | 0.90 | 1.10 | 1.10 |
| | | 1.15 | 1.20 | 1.05 | 0.90 | 0.80 | 1.00 | 1.10 | 0.90 | 1.00 | 0.95 | 0.90 | 1.10 |
| 12 | | 1.20 | 1.20 | 1.10 | 1.00 | 1.00 | 1.00 | 1.10 | 1.00 | 1.10 | 1.20 | 1.30 | 1.25 |
| | | 1.20 | 1.15 | 1.20 | 1.00 | 1.05 | 1.15 | 1.20 | 1.15 | 1.10 | 1.20 | 1.25 | 1.20 |
| 16 | | 1.40 | 1.45 | 1.40 | 1.25 | 1.30 | 1.35 | 1.40 | 1.45 | 1.25 | 1.35 | 1.25 | 1.10 |
| | | 1.20 | 1.35 | 1.30 | 1.00 | 1.10 | 1.30 | 1.10 | 1.00 | 1.10 | 1.10 | 1.40 | 1.30 |
| 20 | | 1.70 | 1.50 | 1.30 | 1.15 | 1.10 | 1.30 | 1.50 | 1.45 | 1.00 | 0.90 | 1.60 | 1.50 |
| | | 1.30 | 1.30 | 0.90 | 0.80 | 0.80 | 1.30 | 1.35 | 1.25 | 1.15 | 1.10 | 1.70 | 1.50 |
| 24 | | 1.70 | 1.55 | 1.30 | 1.20 | 1.35 | 1.20 | 1.30 | 1.50 | 1.35 | 1.40 | 1.65 | 1.70 |
| | | 1.40 | 1.45 | 1.35 | 1.05 | 1.20 | 1.10 | 1.20 | 1.10 | 1.00 | 1.10 | 1.30 | 1.50 |
| 28 | | 1.70 | 1.90 | 1.05 | 1.05 | 1.10 | 1.80 | 1.75 | 2.00 | 1.20 | 1.20 | 1.25 | 2.00 |
| | | 1.60 | 1.45 | 1.00 | 1.10 | 0.70 | 1.75 | 1.00 | 1.50 | 1.15 | 1.10 | 1.45 | 2.00 |

(continued)

Table 10. (Continued)

| Frame No. | Frame Station | Vapor Bubble Projected Diameter - Centimeters | | | | | | | | | | | |
|---|---|---|---|---|---|---|---|---|---|---|---|---|---|
| | | 1 | 2 | 3 | 4 | 5 | 6 | 7 | 8 | 9 | 10 | 11 | 12 |
| | | 13 | 14 | 15 | 16 | 17 | 18 | 19 | 20 | 21 | 22 | 23 | 24 |
| 32 | | 2.00 | 1.90 | 1.30 | 1.70 | 1.40 | 1.15 | 1.90 | 1.10 | 1.20 | 1.15 | 1.20 | 1.75 |
| | | 1.50 | 1.00 | 0.90 | 1.40 | 1.30 | 1.00 | 1.30 | 1.70 | 1.70 | 1.00 | 2.00 | 2.40 |
| 36 | | 1.90 | 1.95 | 1.05 | 1.35 | 1.20 | 1.50 | 1.90 | 1.20 | 1.00 | 1.00 | 1.10 | 1.50 |
| | | 2.25 | 0.90 | 0.80 | 1.50 | 1.55 | 1.00 | 1.15 | 2.30 | 1.65 | 1.30 | 2.10 | 1.70 |
| 40 | | 2.05 | 2.00 | 1.20 | 1.20 | 1.30 | 1.30 | 1.75 | 1.20 | 1.15 | 1.10 | 1.10 | 2.25 |
| | | 2.30 | 1.40 | 0.90 | 1.60 | 1.70 | 1.00 | 1.30 | 1.50 | 1.30 | 1.25 | 2.10 | 1.40 |

Framing Speed: 51 frames = 12 milliseconds

Table 11. Film Growth Rate Data for Run Number 23

| Frame No. | Frame Station | Vapor Bubble Projected Diameter - Centimeters | | | | | | | | | | | |
|---|---|---|---|---|---|---|---|---|---|---|---|---|---|
| | | 1 | 2 | 3 | 4 | 5 | 6 | 7 | 8 | 9 | 10 | 11 | 12 |
| | | 13 | 14 | 15 | 16 | 17 | 18 | 19 | 20 | 21 | 22 | 23 | 24 |
| wire | | 0.70 | 0.70 | 0.70 | 0.70 | 0.65 | 0.70 | 0.70 | 0.70 | 0.65 | 0.70 | 0.70 | 0.70 |
| 4 | | 1.30 | 1.00 | 1.00 | 1.20 | 1.50 | 1.40 | 1.20 | 1.30 | 1.90 | 1.30 | 1.00 | 1.05 |
| | | 1.00 | 1.30 | 0.90 | 1.00 | 0.90 | 0.80 | 1.20 | 1.05 | 1.40 | 1.10 | 1.20 | |
| 8 | | 1.90 | 1.65 | 1.50 | 1.40 | 1.15 | 1.15 | 1.30 | 1.20 | 1.10 | 1.00 | 1.30 | 1.10 |
| | | 1.15 | 1.30 | 1.35 | 1.45 | 1.25 | 1.00 | 1.20 | 1.20 | 1.35 | 1.20 | | |
| 12 | | 2.00 | 2.10 | 1.60 | 1.60 | 1.15 | 1.65 | 1.20 | 1.00 | 1.35 | 1.00 | 1.30 | 1.10 |
| | | 1.20 | 1.25 | 1.50 | 1.10 | 1.30 | 1.25 | 1.05 | 1.15 | 1.45 | | | |
| 16 | | 2.50 | 2.15 | 1.85 | 1.50 | 1.30 | 1.20 | 1.70 | 1.60 | 1.25 | 1.10 | 1.70 | 1.55 |
| | | 1.20 | 2.00 | 1.40 | 1.00 | 1.50 | 2.05 | 1.20 | 1.50 | | | | |
| 20 | | 2.00 | 2.00 | 1.85 | 1.20 | 1.30 | 1.10 | 2.00 | 2.20 | 1.20 | 1.00 | 1.20 | 1.80 |
| | | 1.50 | 1.80 | 1.05 | 1.15 | 1.10 | 2.30 | 2.00 | 1.30 | | | | |
| 24 | | 2.30 | 1.50 | 1.25 | 1.00 | 1.20 | 1.50 | 2.00 | 1.00 | 1.20 | 1.00 | 2.10 | 2.30 |
| | | 1.00 | 1.40 | 1.00 | 1.80 | 2.35 | 1.50 | 1.45 | 2.00 | 2.05 | 1.15 | | |
| 28 | | 2.00 | 2.40 | 1.50 | 1.20 | 1.35 | 1.15 | 1.60 | 1.90 | 1.20 | 1.20 | 2.20 | 1.80 |
| | | 1.70 | 1.75 | 1.20 | 1.10 | 1.80 | 2.00 | 1.05 | 2.40 | | | | |

(continued)

Table 11. (Continued)

| Frame No. | Frame Station | Vapor Bubble Projected Diameter - Centimeters | | | | | | | | | | | |
|---|---|---|---|---|---|---|---|---|---|---|---|---|---|
| | | 1 | 2 | 3 | 4 | 5 | 6 | 7 | 8 | 9 | 10 | 11 | 12 |
| | | 13 | 14 | 15 | 16 | 17 | 18 | 19 | 20 | 21 | 22 | 23 | 24 |
| 32 | | 2.10 | 2.10 | 1.70 | 1.80 | 2.05 | 1.90 | 1.85 | 1.80 | 1.35 | 1.10 | 1.10 | 1.90 |
| | | 1.85 | 1.05 | 1.90 | 1.20 | 1.30 | 2.25 | 1.20 | 1.10 | 2.00 | 1.70 | | |
| 36 | | 2.50 | 2.35 | 2.00 | 1.30 | 1.15 | 1.00 | 2.30 | 2.25 | 1.20 | 1.10 | 1.40 | 1.95 |
| | | 2.05 | 1.15 | 1.20 | 1.10 | 1.20 | 2.20 | 1.70 | 1.60 | 2.10 | 1.55 | | |
| 40 | | 1.50 | 2.90 | 2.30 | 1.20 | 1.10 | 1.10 | 2.10 | 2.10 | 1.20 | 0.90 | 1.20 | 2.00 |
| | | 2.10 | 1.60 | 1.45 | 1.30 | 1.50 | 3.20 | 2.30 | 2.00 | 1.50 | 1.20 | | |

Framing Speed: 53 frames = 13 milliseconds

Table 12. Film Growth Rate Data for Run Number 27

| Frame No. | Frame Station | Vapor Bubble Projected Diameter - Centimeters | | | | | | | | | | | |
|---|---|---|---|---|---|---|---|---|---|---|---|---|---|
| | | 1 | 2 | 3 | 4 | 5 | 6 | 7 | 8 | 9 | 10 | 11 | 12 |
| | | 13 | 14 | 15 | 16 | 17 | 18 | 19 | 20 | 21 | 22 | 23 | 24 |
| wire | | 0.65 | 0.60 | 0.60 | 0.65 | 0.60 | 0.65 | 0.60 | 0.60 | 0.60 | 0.60 | 0.60 | 0.65 |
| 4 | | 0.75 | 1.00 | 0.95 | 0.75 | 1.05 | 0.90 | 0.80 | 0.65 | 0.85 | 0.80 | 0.80 | 0.75 |
| | | 0.80 | 0.65 | 1.20 | 1.05 | 0.90 | 0.80 | 0.65 | 0.70 | 0.70 | 1.00 | 0.90 | 0.75 |
| 8 | | 1.20 | 1.25 | 1.00 | 1.05 | 1.15 | 0.70 | 1.10 | 0.65 | 0.80 | 1.15 | 1.25 | 1.20 |
| | | 0.90 | 0.70 | 0.90 | 0.70 | 0.80 | 1.05 | 1.00 | 0.80 | 1.05 | 0.70 | 1.00 | 1.30 |
| 12 | | 1.30 | 1.35 | 1.10 | 1.75 | 0.85 | 1.10 | 0.90 | 1.30 | 0.70 | 0.85 | 1.30 | 1.50 |
| | | 1.35 | 0.70 | 0.85 | 1.10 | 1.00 | 0.70 | 1.35 | 1.15 | 0.70 | 1.25 | 0.75 | 1.55 |
| 16 | | 1.70 | 1.50 | 1.20 | 1.00 | 1.55 | 1.25 | 1.00 | 0.90 | 0.85 | 1.05 | 1.75 | 1.35 |
| | | 0.70 | 0.70 | 0.95 | 1.20 | 0.65 | 1.30 | 1.30 | 0.65 | 1.50 | 1.00 | 0.70 | 1.60 |
| 20 | | 1.90 | 2.05 | 0.70 | 0.75 | 1.40 | 1.30 | 1.00 | 0.85 | 1.25 | 0.65 | 2.30 | 0.70 |
| | | 0.65 | 0.70 | 1.35 | 1.70 | 0.80 | 1.20 | 1.05 | 0.85 | 1.50 | 1.25 | 1.10 | 1.40 |
| 24 | | 1.95 | 1.80 | 0.75 | 1.20 | 1.60 | 1.40 | 0.90 | 1.50 | 1.65 | 1.15 | 1.30 | 1.50 |
| | | 1.20 | 0.90 | 1.50 | 1.30 | 0.80 | 1.80 | 1.30 | 0.80 | 1.85 | 1.00 | 1.60 | 1.95 |
| 28 | | 2.25 | 1.50 | 0.80 | 0.85 | 1.65 | 2.00 | 0.75 | 1.50 | 1.00 | 1.65 | 1.50 | 1.50 |
| | | 1.00 | 0.70 | 1.80 | 1.50 | 1.00 | 1.50 | 1.05 | 0.90 | 1.80 | 1.15 | 1.50 | 1.80 |

(continued)

Table 12. (Continued)

| Frame No. | Frame Station | Vapor Bubble Projected Diameter - Centimeters | | | | | | | | | | | |
|---|---|---|---|---|---|---|---|---|---|---|---|---|---|
| | | 1 | 2 | 3 | 4 | 5 | 6 | 7 | 8 | 9 | 10 | 11 | 12 |
| | | 13 | 14 | 15 | 16 | 17 | 18 | 19 | 20 | 21 | 22 | 23 | 24 |
| 32 | | 2.30 | 2.00 | 1.05 | 0.80 | 1.35 | 2.35 | 1.20 | 1.20 | 1.65 | 0.75 | 2.00 | 1.05 |
| | | 0.80 | 0.70 | 1.75 | 1.70 | 0.65 | 1.30 | 1.50 | 0.70 | 1.35 | 1.30 | 1.85 | 1.70 |
| 36 | | 2.10 | 2.25 | 0.90 | 1.00 | 1.85 | 1.90 | 0.70 | 1.00 | 1.50 | 1.50 | 1.05 | 1.90 |
| | | 1.45 | 1.00 | 1.55 | 1.60 | 0.70 | 1.70 | 1.70 | 0.75 | 1.90 | 1.60 | 0.80 | 2.10 |
| 40 | | 2.20 | 2.05 | 1.50 | 1.00 | 1.80 | 1.80 | 0.70 | 1.50 | 1.80 | 1.05 | 1.80 | 1.60 |
| | | 1.10 | 0.80 | 1.40 | 1.75 | 1.90 | 1.20 | 1.15 | 1.00 | 1.95 | 1.60 | 1.20 | 2.00 |

Framing Speed: 39.5 frames = 10 milliseconds

Table 13. Film Growth Rate Data for Run Number 29

| Frame No. | Frame Station | Vapor Bubble Projected Diameter - Centimeters | | | | | | | | | | | |
|---|---|---|---|---|---|---|---|---|---|---|---|---|---|
| | | 1 | 2 | 3 | 4 | 5 | 6 | 7 | 8 | 9 | 10 | 11 | 12 |
| | | 13 | 14 | 15 | 16 | 17 | 18 | 19 | 20 | 21 | 22 | 23 | 24 |
| wire | | 0.65 | 0.65 | 0.60 | 0.65 | 0.60 | 0.60 | | | | | | |
| 4 | | 1.90 | 1.65 | 1.55 | 1.45 | 1.85 | 1.80 | 1.20 | 1.15 | 0.90 | 1.60 | 1.40 | 1.25 |
| | | 1.70 | 0.80 | 1.70 | 1.30 | 1.15 | 1.30 | 1.55 | 1.45 | 1.25 | 1.95 | 1.50 | 1.70 |
| 8 | | 2.25 | 1.85 | 1.65 | 1.50 | 2.00 | 2.55 | 2.15 | 0.80 | 1.30 | 2.15 | 1.60 | 1.75 |
| | | 0.80 | 1.70 | 2.30 | 1.05 | 1.65 | 1.70 | 1.20 | 1.75 | 1.80 | 1.60 | 1.45 | 2.00 |
| 12 | | 2.35 | 2.15 | 1.05 | 1.35 | 2.30 | 2.95 | 1.90 | 0.90 | 2.05 | 2.05 | 2.30 | 2.20 |
| | | 0.80 | 2.25 | 2.70 | 1.35 | 1.55 | 2.10 | 2.10 | 2.00 | 2.15 | 1.20 | 1.75 | 3.00 |
| 16 | | 3.10 | 2.00 | 1.15 | 1.25 | 3.10 | 2.95 | 1.20 | 0.90 | 1.50 | 3.15 | 2.75 | 1.10 |
| | | 0.95 | 2.50 | 2.70 | 1.35 | 1.65 | 2.40 | 1.50 | 2.40 | 1.30 | 0.80 | 1.50 | 3.00 |
| 20 | | 3.65 | 2.50 | 0.85 | 1.50 | 2.90 | 3.20 | 1.05 | 0.80 | 1.10 | 3.35 | 3.00 | 1.30 |
| | | 0.80 | 2.15 | 2.90 | 2.15 | 0.75 | 1.70 | 2.70 | 1.35 | 1.50 | 1.00 | 2.90 | 3.15 |
| 24 | | 3.25 | 3.00 | 0.90 | 1.00 | 3.35 | 3.20 | 1.60 | 1.20 | 1.00 | 3.35 | 3.40 | 1.40 |
| | | 0.90 | 2.35 | 2.80 | 1.90 | 0.90 | 2.10 | 2.50 | 2.20 | 1.35 | 0.95 | 2.15 | 3.20 |
| 28 | | 3.75 | 2.50 | 0.85 | 1.00 | 2.80 | 3.35 | 2.10 | 0.90 | 1.00 | 2.70 | 3.75 | 2.00 |
| | | 0.80 | 1.80 | 2.85 | 2.50 | 0.75 | 1.70 | 3.10 | 2.85 | 0.90 | 0.80 | 2.55 | 3.20 |

(continued)

Table 13. (Continued)

| Frame No. | Frame Station | Vapor Bubble Projected Diameter - Centimeters | | | | | | | | | | | |
|---|---|---|---|---|---|---|---|---|---|---|---|---|---|
| | | 1 | 2 | 3 | 4 | 5 | 6 | 7 | 8 | 9 | 10 | 11 | 12 |
| | | 13 | 14 | 15 | 16 | 17 | 18 | 19 | 20 | 21 | 22 | 23 | 24 |
| 32 | | 3.60 | 3.20 | 1.50 | 2.65 | 3.00 | 3.20 | 2.05 | 0.90 | 2.10 | 3.20 | 3.45 | 1.50 |
| | | 0.70 | 1.50 | 2.95 | 2.50 | 0.80 | 1.70 | 3.60 | 2.10 | 0.80 | 1.55 | 2.80 | 3.35 |
| 36 | | 3.60 | 2.30 | 1.10 | 2.65 | 3.50 | 3.20 | 1.80 | 0.90 | 2.25 | 3.55 | 3.60 | 1.80 |
| | | 0.85 | 2.00 | 3.45 | 2.15 | 0.90 | 3.00 | 3.20 | 2.20 | 0.90 | 1.35 | 3.05 | 3.95 |
| 40 | | 3.50 | 2.50 | 1.30 | 1.55 | 3.50 | 3.40 | 2.00 | 0.95 | 2.00 | 3.45 | 3.50 | 2.65 |
| | | 1.05 | 1.90 | 3.50 | 2.75 | 1.00 | 2.95 | 3.40 | 2.50 | 1.20 | 1.70 | 2.50 | 4.00 |

Framing Speed: 52 frames = 13 milliseconds

Table 14. Film Growth Rate Data for Run Number 30

| Frame No. | Frame Station | Vapor Bubble Projected Diameter - Centimeters | | | | | | | | | | | |
|---|---|---|---|---|---|---|---|---|---|---|---|---|---|
| | | 1 | 2 | 3 | 4 | 5 | 6 | 7 | 8 | 9 | 10 | 11 | 12 |
| | | 13 | 14 | 15 | 16 | 17 | 18 | 19 | 20 | 21 | 22 | 23 | 24 |
| wire | | 0.55 | 0.55 | 0.55 | 0.55 | 0.50 | 0.55 | 0.55 | 0.60 | 0.55 | 0.55 | 0.55 | |
| 4 | | 1.20 | 1.30 | 1.70 | 1.15 | 1.05 | 1.00 | 1.25 | 1.00 | 1.15 | 0.70 | 0.65 | 1.50 |
| | | 1.50 | 0.70 | 1.15 | 0.80 | 1.15 | 1.30 | 1.10 | 0.95 | 1.00 | 1.30 | 1.00 | 1.35 |
| 8 | | 1.30 | 1.50 | 1.45 | 0.70 | 0.75 | 1.20 | 1.30 | 1.25 | 1.10 | 0.70 | 1.35 | 1.50 |
| | | 1.40 | 0.80 | 0.95 | 0.75 | 0.85 | 1.15 | 1.00 | 1.10 | 0.70 | 1.00 | 0.95 | 1.60 |
| 12 | | 0.90 | 1.75 | 1.10 | 0.80 | 0.70 | 1.10 | 1.55 | 1.90 | 1.30 | 0.85 | 1.55 | 1.70 |
| | | 1.25 | 1.05 | 0.80 | 0.70 | 0.85 | 1.40 | 1.60 | 0.90 | 0.70 | 1.05 | 1.40 | 1.70 |
| 16 | | 0.90 | 2.15 | 1.50 | 1.20 | 0.90 | 0.80 | 2.20 | 2.05 | 0.90 | 1.15 | 1.60 | 1.10 |
| | | 2.10 | 1.00 | 0.90 | 0.70 | 0.75 | 1.80 | 2.20 | 0.80 | 1.05 | 0.80 | 1.95 | 1.80 |
| 20 | | 0.95 | 1.90 | 1.95 | 1.15 | 1.85 | 0.90 | 1.50 | 2.50 | 0.85 | 1.10 | 1.50 | 0.70 |
| | | 1.70 | 1.45 | 0.80 | 1.55 | 0.65 | 1.50 | 1.85 | 1.30 | 1.40 | 0.80 | 1.70 | 1.60 |
| 24 | | 1.25 | 2.05 | 2.20 | 0.95 | 1.50 | 0.85 | 1.15 | 2.70 | 0.80 | 0.85 | 1.15 | 0.75 |
| | | 2.55 | 1.20 | 0.80 | 1.15 | 0.85 | 0.80 | 2.10 | 1.15 | 1.25 | 1.00 | 1.10 | 2.20 |
| 28 | | 0.95 | 1.85 | 2.05 | 2.15 | 1.30 | 1.10 | 1.85 | 1.70 | 1.15 | 1.25 | 1.65 | 1.35 |
| | | 1.00 | 0.65 | 1.55 | 1.35 | 0.80 | 2.00 | 2.00 | 1.10 | 1.50 | 1.00 | 2.15 | 2.30 |

(continued)

Table 14. (Continued)

| Frame No. | Frame Station | Vapor Bubble Projected Diameter - Centimeters | | | | | | | | | | | |
|---|---|---|---|---|---|---|---|---|---|---|---|---|---|
| | | 1 | 2 | 3 | 4 | 5 | 6 | 7 | 8 | 9 | 10 | 11 | 12 |
| | | 13 | 14 | 15 | 16 | 17 | 18 | 19 | 20 | 21 | 22 | 23 | 24 |
| 32 | | 1.35 | 2.25 | 1.75 | 1.85 | 1.60 | 0.90 | 2.20 | 2.25 | 1.20 | 1.55 | 1.50 | 1.40 |
| | | 1.50 | 1.45 | 1.20 | 1.65 | 0.70 | 2.05 | 1.95 | 1.35 | 1.05 | 1.00 | 2.10 | 1.35 |
| 36 | | 1.00 | 2.10 | 2.40 | 2.45 | 0.80 | 1.80 | 1.70 | 1.30 | 0.95 | 1.70 | 2.10 | 1.00 |
| | | 1.80 | 0.70 | 1.40 | 1.35 | 1.00 | 1.25 | 2.35 | 0.80 | 1.20 | 0.80 | 2.00 | 2.40 |
| 40 | | 1.40 | 2.00 | 2.70 | 1.35 | 1.20 | 0.90 | 2.05 | 2.05 | 1.25 | 0.90 | 2.10 | 1.50 |
| | | 0.85 | 0.65 | 2.00 | 1.80 | 0.70 | 2.00 | 2.25 | 0.90 | 1.20 | 1.00 | 2.70 | 2.00 |

Framing Speed: 44 frames = 11 milliseconds

Table 15. Film Growth Rate Data for Run Number 32

| Frame No. | Frame Station | Vapor Bubble Projected Diameter - Centimeters | | | | | | | | | | | |
|---|---|---|---|---|---|---|---|---|---|---|---|---|---|
| | | 1 | 2 | 3 | 4 | 5 | 6 | 7 | 8 | 9 | 10 | 11 | 12 |
| | | 13 | 14 | 15 | 16 | 17 | 18 | 19 | 20 | 21 | 22 | 23 | 24 |
| wire | | 0.85 | 0.80 | 0.80 | 0.75 | 0.75 | 0.70 | 0.70 | 0.70 | 0.70 | 0.70 | 0.70 | 0.70 |
| | | 0.70 | 0.70 | | | | | | | | | | |
| 4 | | 1.05 | 1.15 | 1.15 | 1.20 | 1.10 | 1.00 | 0.90 | 1.00 | 0.90 | 0.85 | 1.05 | 1.10 |
| | | 1.00 | 1.25 | 1.10 | 0.90 | 1.00 | 1.00 | 1.00 | 0.95 | 1.10 | 1.00 | 1.10 | 0.85 |
| 8 | | 1.50 | 1.45 | 1.50 | 1.30 | 1.35 | 1.10 | 1.05 | 1.15 | 0.95 | 1.05 | 1.10 | 0.80 |
| | | 0.90 | 1.10 | 1.20 | 1.25 | 1.00 | 0.95 | 1.15 | 1.05 | 1.00 | 0.90 | 1.00 | 1.30 |
| 12 | | 1.35 | 1.30 | 1.30 | 1.15 | 1.10 | 1.20 | 1.70 | 1.05 | 0.90 | 1.20 | 1.10 | 0.80 |
| | | 0.85 | 1.00 | 0.80 | 1.10 | | | | | | | | |
| 16 | | 1.55 | 1.40 | 1.40 | 1.55 | 1.25 | 1.00 | 0.95 | 1.00 | 0.80 | 0.75 | 1.10 | 1.05 |
| | | 0.85 | 0.95 | 1.20 | 1.20 | 1.40 | 1.25 | 1.00 | | | | | |
| 20 | | 1.25 | 1.20 | 1.30 | 1.35 | 1.10 | 1.30 | 1.35 | 1.10 | 1.05 | 1.10 | 1.10 | 0.90 |
| | | 1.20 | 1.20 | 1.10 | 1.10 | 1.15 | 1.10 | | | | | | |
| 24 | | 1.70 | 1.35 | 1.40 | 1.35 | 1.30 | 1.25 | 1.20 | 1.00 | 1.05 | 1.00 | 0.95 | 1.10 |
| | | 1.30 | 0.90 | 0.95 | 1.00 | 1.05 | 1.05 | 1.00 | 1.10 | | | | |
| 28 | | 1.40 | 1.30 | 1.55 | 1.50 | 0.95 | 1.40 | 1.40 | 1.30 | 0.95 | 1.10 | 1.30 | 1.00 |
| | | 1.00 | 0.80 | 0.90 | 0.85 | 1.30 | 1.40 | 1.00 | | | | | |

(continued)

Table 15. (Continued)

| Frame No. | Frame Station | Vapor Bubble Projected Diameter - Centimeters | | | | | | | | | | | |
|---|---|---|---|---|---|---|---|---|---|---|---|---|---|
| | | 1 | 2 | 3 | 4 | 5 | 6 | 7 | 8 | 9 | 10 | 11 | 12 |
| | | 13 | 14 | 15 | 16 | 17 | 18 | 19 | 20 | 21 | 22 | 23 | 24 |
| 32 | | 1.70 | 1.65 | 1.45 | 1.35 | 1.35 | 1.35 | 1.55 | 1.20 | 0.95 | 1.05 | 0.90 | 1.10 |
| | | 1.15 | 1.00 | 1.05 | 0.85 | 0.80 | 1.20 | 1.10 | 1.05 | 1.65 | 1.75 | 1.25 | |
| 36 | | 1.60 | 1.70 | 1.30 | 1.35 | 1.35 | 1.65 | 1.90 | 1.00 | 1.05 | 1.10 | 1.05 | 1.10 |
| | | 1.00 | 0.95 | 0.80 | 1.10 | 1.15 | 1.20 | 1.55 | 0.90 | 1.15 | 1.95 | 1.15 | |
| 40 | | 1.70 | 1.85 | 1.45 | 1.55 | 1.45 | 1.50 | 1.55 | 1.25 | 1.35 | 1.60 | 1.30 | 1.35 |
| | | 1.15 | 1.80 | 1.00 | 1.10 | 1.80 | 0.90 | 1.75 | 0.80 | | | | |

Framing Speed: 41 frames = 10 milliseconds

# BIBLIOGRAPHY


1. S. Nukiyama, "Maximum and Minimum Values of Heat Transmitted from Metal to Boiling Water Under Atmospheric Pressure," Journal of the Society of Mechanical Engineers, Japan 37, 367 (1934).

2. N. W. Snyder, "Summary of Conference on Bubble Dynamics and Boiling Heat Transfer Held at the Jet Propulsion Laboratory, June 14 and 15, 1956," ed. by S. G. Bankoff, W. J. Colahan, Jr., and D. R. Bartz, Jet Propulsion Laboratory Memo No. 20-137, California Institute of Technology, December 10, 1956.

3. T. T. Robin, Jr., "Mass Transfer Effects in Subcooled Nucleate Boiling," Ph.D. Thesis, School of Nuclear Engineering, Georgia Institute of Technology, November, 1966.

4. M. Jakob, Heat Transfer, Volume I, John Wiley & Sons, Inc. New York, 1949.

5. F. Kreith, Principles of Heat Transfer, International Textbook Company, Scranton, Pennsylvania, 1958.

6. W. H. McAdams, Heat Transmission, 3rd ed., McGraw-Hill Book Company, Inc., New York, 1954.

7. L. S. Tong, Boiling Heat Transfer and Two-Phase Flow, John Wiley & Sons, Inc., New York, 1965.

8. R. Cole, "Investigation of Transient Pool Boiling Due to Sudden Large Power Surge," NACA TN-3885, December, 1956.

9. E. A. McLean, V. E. Scherrer, and C. E. Faneuff, "Film Boiling of Water by Pulse-Heating Small Wire," Journal of Applied Physics 27, 193 (1956).

10. M. W. Rosenthal and R. L. Miller, "An Experimental Study of Transient Boiling," ORNL-2294, Oak Ridge National Laboratory (1957).

11. T. D. Hamill and S. G. Bankoff, "Growth of a Vapor Film at a Rapidly Heated Plane Surface," Chemical Engineering Science 18, 355 (1963).

12. T. D. Hamill and S. G. Bankoff, "Maximum and Minimum Bounds for the Growth of a Vapor Film at the Surface of a Rapidly Heated Plate," Chemical Engineering Science 19, 59 (1964).

13. H. A. Johnson, V. E. Schrock, F. B. Selph, J. H. Lienhard, and Z. R. Rosztoczy, "Transient Pool Boiling of Water at Atmospheric Pressure," International Developments in Heat Transfer, Heat Transfer Conference, Boulder, Colorado, American Society of Mechanical Engineers, August 28 - September 1, 1961. 244.

14. H. Laurie and H. A. Johnson, "Transient Pool Boiling of Water on a Vertical Surface with a Step Change in Heat Generation," Transactions of the American Society of Mechanical Engineers, Series C, Journal of Heat Transfer 84, No. 3, 217 (1962).

15. R. W. Graham, "Experimental Observations of Transient Boiling of Subcooled Water and Alcohol on a Horizontal Surface," National Aeronautics and Space Administration Technical Note D-2507, January, 1965.

16. D. R. Pitts, "Transient Film Boiling on a Horizontal Cylindrical Surface," Ph.D. Thesis, School of Mechanical Engineering, Georgia Institute of Technology, August, 1967.

17. L. A. Bromley, "Heat Transfer in Stable Film Boiling," Chemical Engineering Progress 46, No. 5, 221-226 (1950).

18. H. S. Carslaw and J. C. Jaeger, Conduction of Heat in Solids, Oxford University Press, London, 1959.

19. J. H. Keenan and F. G. Keyes, Thermodynamic Properties of Steam, John Wiley & Sons, Inc., New York, 1936.

20. K. Pearson, Tables of the Incomplete Γ-Function, Cambridge University Press, London, 1946.

21. M. Abramowitz and I. A. Stegun, Handbook of Mathematical Functions, U. S. Government Printing Office, Washington, D. C., 1964.

# VITA

Howard Hong-Yuang Yen was born in Taipei, Taiwan, China on May 18, 1937. He graduated from Chen-Kuo High School in Taipei, Taiwan in June, 1956. He entered National Taiwan University in September, 1956, and graduated in June, 1960, receiving a Bachelor of Science degree in Mechanical Engineering.

Following graduation, he entered active duty in the Chinese Navy, where he served for two years as an engineering officer.

After this, he came to the United States and began his graduate study at the Georgia Institute of Technology in 1962, with the aid of a Rotary Club fellowship, and received the degree, Master of Science in Mechanical Engineering in 1964. From 1963 to 1966 he worked at the Heat Technology Laboratory in Huntsville, Alabama. He returned to the Georgia Institute of Technology in 1966 to pursue the doctorate in Mechanical Engineering.

Mr. Yen was married in 1964 to the former Miss Frances Lee-Hwa Lee. They have two children, David Hun-Kuan and Audrey Sheau-Ru.